THE ROLE OF TISSUE TRANSGLUTAMINASE IN KIDNEY CANCER

by
Merve ERDEM

Submitted to the Institute of Graduate Studies in
Science and Engineering in partial fulfillment of
the requirements for the degree of
Master of Science
in
Biotechnology

Yeditepe University
2011

THE ROLE OF TISSUE TRANSGLUTAMINASE IN KIDNEY CANCER

APPROVED BY:

Asst. Prof. Dilek TELCİ .....
(Thesis Supervisor)

Dr. Öner ŞANLI .....

Assoc. Prof. Gamze KÖSE .....

Asst. Prof. Elif Damla ARISAN .....

DATE OF APPROVAL: …./…./….

ACKNOWLEDGEMENTS

I would like to express my deep gratitude to my supervisor Asst. Prof. Dilek Telci for her support, guidance, and invaluable advice throughout my research period. I also wish to express my gratitude Prof. Fikrettin Şahin for his continuous support and invaluable advice whenever I needed.

I would like to express my great appreciation to my lab partners Ayca Zeynep İlter and Nihan Kılınç and trainee student Eray Şahin for their help in the experiments and support. I would like to thank to Siğnem Eyüboğlu for her understanding and help during my thesis.

I would like to thank Dr. Öner Şanlı and Dr. Selçuk Erdem who provided the patient tissue samples for the study.

I would also like to thank my friends especially Melis Uslu, Pınar Atalay, Selami Demirci, İsmail Sayın, Safa Aydın, Dilek Mercan and Mehmet Emir Yalvaç for their continuous support and understanding whenever I needed.

Finally, I would like to express my deepest gratitude to my parents İsmail Erdem and Züleyha Erdem for their endless love, patience, and their confidence in me. I am also thankful to the other members of my family, Tuba Erdem Koç and Safa Erdem for making my life more pleasurable.

ABSTRACT

THE ROLE OF TISSUE TRANSGLUTAMINASE IN KIDNEY CANCER

Tissue transglutaminase (TG2) is a ubiquitously expressed enzyme and has versatile functions in extracellular matrix (ECM)-stabilization, cell adhesion and cell survival. Different from the enzymatic activity, TG2 may behave as a cell adhesion signaling molecule via binding to syndecan-4 heparan sulfate proteoglycan and favor integrin β1-dependent signaling resulting in the maintenance of cell adhesion and cell survival. Early studies suggested that TG2 activity and expression decrease in the primary tumors resulting in ECM destabilization. However, increased TG2 expression in parallel with β1 integrin contributing to the drug resistance, was reported in the metastatic tumors.

Renal cell carcinoma (RCC) is the most common type of kidney cancers. This study investigates the importance of TG2 in RCC by analyzing gene expression and enzymatic activity of TG2 in the tissue samples from the RCC patients along with the RCC cell lines. The results indicated that 34% of RCC tumor tissues showed increased TG2 expression compared to the healthy tissues. Moreover, in 71% of these increased TG2 expression was found to be in parallel with the increased syndecan-4 and integrin β1 levels. TG2 activity assay results showed that TG2 activity was decreased in most of the tumors. Given that TG2 acts as a matrix-stabilizer, the decreased TG2 activity may subject the stroma of RCC tumor more susceptible to proteolytic degradation allowing increased tumor growth and angiogenesis. Analysis of RCC cell lines also confirmed the results obtained from the RCC patients. This research is the first study to investigate the significance of TG2 in RCC.

ÖZET

DOKU TRANSGLUTAMİNAZININ BÖBREK KANSERİNDEKİ ROLÜ

Doku transglutaminazı (TG2), her dokuda ifade edilen ve hücre-dışı matrisin sağlamlaştırılması, hücre yapışması ve hücre canlılığında çok yönlü fonksiyon gösteren bir enzimdir. TG2, enzimatik aktivitesinden farklı olarak, sindekan-4 heparan sülfat proteoglikanına bağlanarak ve integrin β1 bağımlı hücre yapışması ve hücre canlılığı sinyalizasyonunu destekleyerek, hücre yapışması sinyal molekülü olarak görev yapar. Daha önceki çalışmalar, TG2 aktivite ve ifadesinin, primer tümörlerde azaldığını ve bunun hücre-dışı matris yapısını gevşettiğini öne sürmüştür. Buna karşın metastatik tümörlerde TG2 ifadesinin, β1 integrin ile paralel artışının ilaç dirençliliğine katkıda bulunduğu gösterilmiştir.

Böbrek hücreli karsinom (BHK), böbrek kanserinin en yaygın görülen tipidir. Bu çalışma; TG2'nin BHK'daki önemini, gen ifadesi ve TG2'nin enzim aktivitesi açısından, BHK hastalarından alınan doku örneklerinde ve BHK hücre hatlarında incelemektedir. BHK tümör dokuları sağlıklı dokularla karşılaştırıldığında, BHK tümörlerinin %34'ünde TG2 ifadesinin artmış olduğu tespit edilmiştir. Ayrıca artmış TG2 ifadesi gösteren hastaların %71'inde, sindekan-4 ve β1 integrin ifadelerinde paralel bir artış görülmüştür. TG2 aktivite testi sonuçları, TG2'nin aktivitesinin çoğu dokuda düştüğünü göstermiştir. TG2 enziminin matris sağlamlaştırıcısı olarak görev yaptığı göz önünde tutulduğunda, azalmış TG2 aktivitesinin, BHK tümör stromasının proteolitik yıkımla gevşemesine sebebiyet vererek tümör büyümesi ve damarlanmayla sonuçlanması olasıdır. BHK hücre hatları da BHK hastalarından aldığımız sonuçlarımızı doğrulamıştır. Bu çalışma TG2'nin BHK'deki önemini inceleyen ilk çalışmadır.

TABLE OF CONTENTS

LIST OF FIGURES

LIST OF TABLES

LIST OF SYMBOLS / ABBREVIATIONS

APS	Ammonium persulfate
ATCC	American Type Culture Collection
ATP	Adenosine triphosphate
BSA	Bovine serum albumin
BTC	Biotin cadaverine, trifluoroacetate salt (N-(5-aminopentyl) biotinamide, trifluoroacetic acid salt)
Ca^{2+}	Free calcium ion
cDNA	Complementary deoxyribonucleic acid
DMEM	Dulbecco's Modified Eagle Medium
DMSO	Dimethylsulfoxide
DTT	Dithiothreitol
ECM	Extracellular matrix
EDTA	Ethylenediaminetetraacetic acid
FAK	Focal adhesion kinase
FN	Fibronectin
GTP	Guanosine triphosphate
HRP	Horse-radish peroxidase
ITGB1	Integrin β1
M	Molar
ml	Milliliters
µl	Microliters
mM	Milimolar
MMP	Matrix metalloproteinases
ng	Nanogram
nM	Nanomolar
pH	Negative log of hydrogen ion concentration
PKCα	Protein kinase C α
RCC	Renal cell carcinoma
RNA	Ribonucleic acid
RPTEC	Renal proximal tubule epithelial cells

RTCC	Renal transitional cell carcinoma
S.D.	Standard deviation
SDC-4	Syndecan-4
SDS-PAGE	Sodium Dodecyl Sulfate Polyacrylamide Gel Electrophoresis
TEMED	N,N,N′,N′-Tetramethylethylenediamine
TG2	Tissue trasnglutaminase
TGF-β	Transforming growth factor-β
TIMP	Tissue inhibitors of metalloproteinases
TMB	3,3’,5,5’-Tetramethyl benzidine
Wt1	Wilms tumor protein

1. INTRODUCTION

1.1. KIDNEY PHYSIOLOGY

Kidneys are organs located at the back of the abdominal cavity, at each side of the vertebral coloumn. Kidney is an organ that comprises diverse specialized cell types arranged in a highly organized three-dimensional pattern. As shown in Figure 1.1, each kidney has parenchyma and collecting system; parenchyma contains cortex and medulla, and the collecting system contains the calyces, renal pelvis and the ureter as shown in Figure 1.1. The functional unit of kidney called nephron is found approximately 600,000 (300,000-1,400,000) in a kidney. This functional unit includes specialized cells that filter the plasma, absorb the filtrate and secrete the substances throughout the urine formation [1].

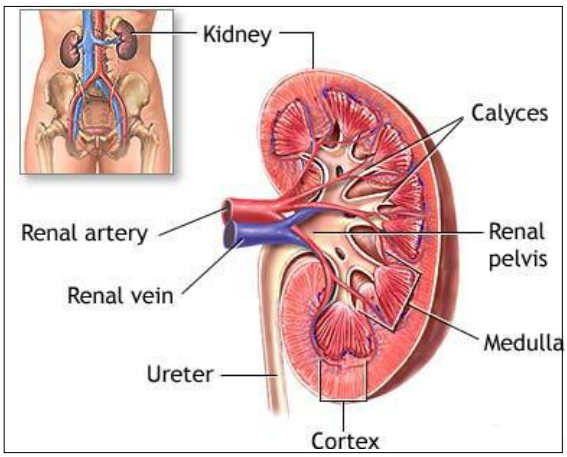

Figure 1.1. Kidney anatomy [2]

The nephron is located both at the outer layer of kidney, cortex and the inner part, medulla as illustrated in Figure 1.2. The cortex contains the renal corpuscle (glomerulus and Bowman's capsule), most part of the proximal tubule and some part of the distal tubule. The medulla includes the loops of Henle, and collecting ducts. The glomerulus is composed of capillaries lined by the endothelial cells, mesengilial cells at the middle of the capillaries and specialized epithelial cells called podocytes surrounding the capillaries [3].

Bowman’s capsule, the double wall wrapping the glomerulus, consists of thin squamous epithelial cells on its outer surface. The proximal tubule has columnar epithelial cells consisting of many microvilli and increased luminal surface area whereas the loop of Henle containing ascending and descending tubules inside the medulla is lined by more thinner and smooth surface epithelial cells. The distal tubule is lined with simple cuboidal cells that are shorter than the proximal tubule cells and similarly collecting duct contains simple cuboidal epithelial cells [1, 4].

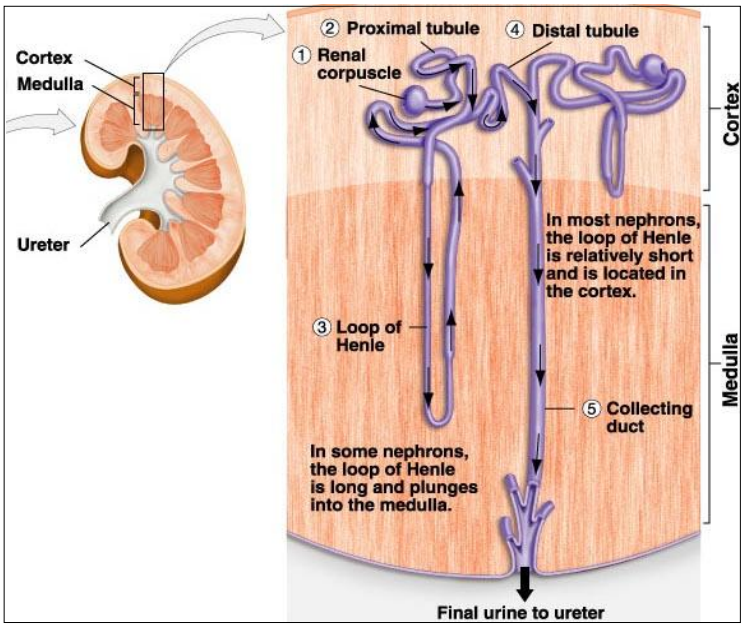

Figure 1.2. A diagram of a nephron [5]

As result of this complicated structure the kidney has important regulatory functions for the body including; i) protection of body composition (regulation of fluid balance in the body, its osmolarity, electrolyte content and concentration, acid-base balance, reabsorption of glucose, amino acids, and other small molecules), ii) removal of metabolic waste products and unknown substances (especially urea, toxins or drugs) and iii) synthesis of enzymes and hormones (renin, erythropoietin and the active form of vitamin D) [3].

1.2. KIDNEY CANCER

Kidney cancer, the cancer that derived from kidneys is mainly classified into two types; the renal cell carcinoma (RCC) which originates from the renal parenchyma and the renal transitional cell carcinoma (RTCC) which originates from the renal pelvis. In children, mostly the nephroblastoma also known as Wilms tumor occurs due to a mutation in transcription factor Wilms tumor protein (Wt1). Investigation of the prevalence in kidney cancer types, showed that RCC generates approximately 90% of kidney cancer and RTCC accounts less than 10% of kidney cancer [6, 7].

Cancer epidemiology studies and statistical analysis report that kidney cancer constitutes approximately 2% of all cancer types in the world with 200,000 new cases and 100,000 deaths every year [8]. According to sexual category, the ratios of kidney cancer in men and women are 2.5% and 1.7%, respectively. In Turkey, kidney cancer rates are similar with these results [9]. In terms of incidence and mortality rates, kidney cancer varies in different regions and populations (Figure 1.3), high in Western and Eastern Europe, North America, Australia and Scandinavia, and low in Asia, Africa and South America [10].

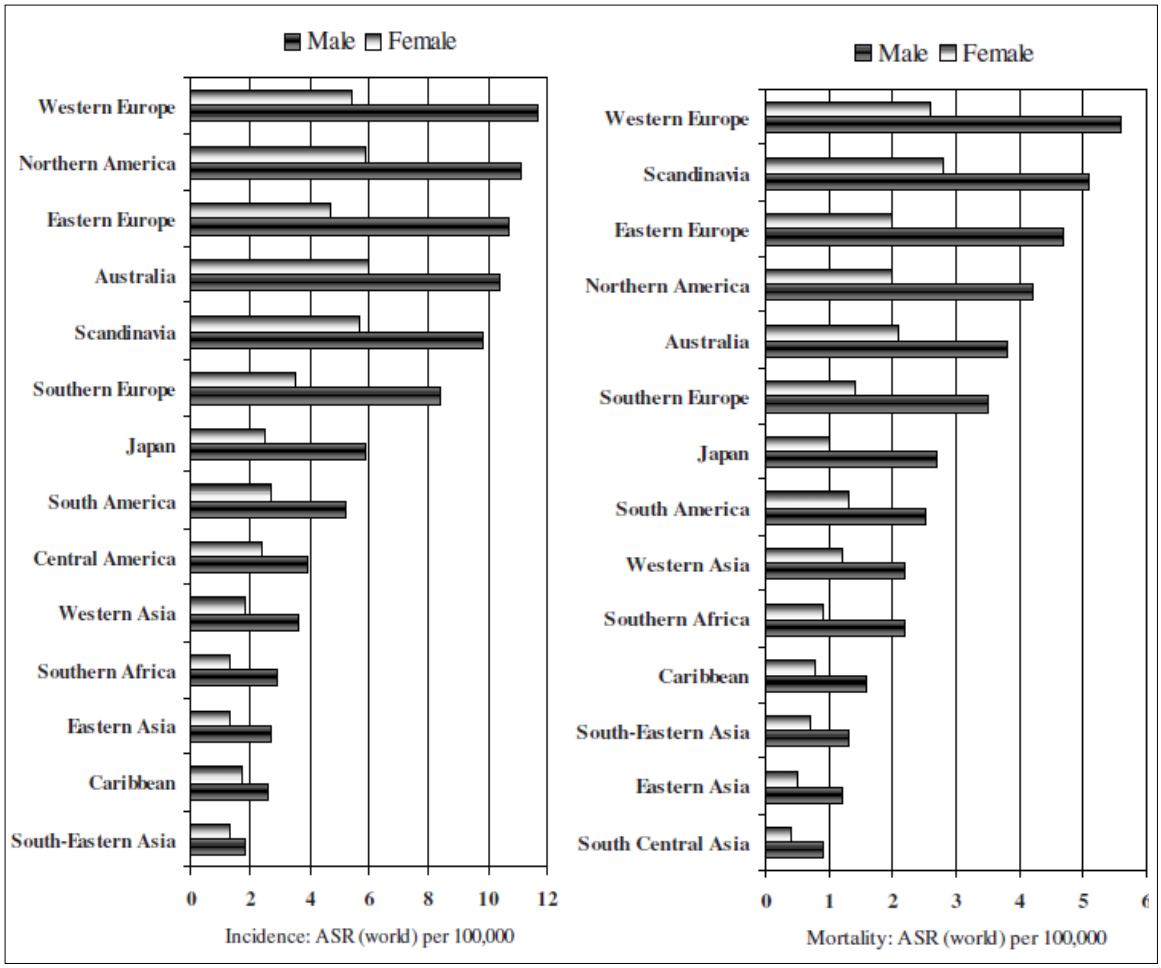

Figure 1.3. Kidney cancer incidence and mortality [10]

1.3. RENAL CELL CARCINOMA

1.3.1. General Description and Statistics

RCC is the common type of kidney carcinoma that comprises 90% of kidney cancer cases. Mortality to incidence ratio of RCC is higher than other urological cancers and is more resistant to radiotherapy and chemotherapy. RCCs arise from renal tubular epithelial cells (most of them are derived from renal epithelial cells of proximal tubular cells) [11]. RCC is divided into four histological subtypes which are conventional (clear cell) RCC, papillary RCC, chromophobe RCC, collecting-duct RCC and unclassified RCC [12]. The most common RCC subtype is the clear cell RCC with a rate of 80-90% of all RCC, and the rates of other types are distributed as papillary RCC 10%, chromophobe RCC 5%, collecting-duct 1% and unclassified types 1% [13, 14].

Grading is one of the most powerful prognostic factors in the management of RCC. Similar to other cancer types, TNM (Tumor, Node, Metastasis) classification is widely used in RCC. This grading system indicating the anatomical extension of tumor, diffusion to regional lymph nodes and distant metastasis is mainly used in RCC as prognostic factor. In addition to this system, Fuhrman nuclear grading system which grades the tumors according to nuclear size, nuclear shape and nucleoli is also used. However, in the prognosis of RCC, TNM classification is accepted as more reliable than Fuhrman grading system in the recent years [15].

1.3.2. Current Therapies of Renal Cell Carcinoma

Today, surgical approach seems the most effective treatment for primary RCC. In the treatment of localized RCC, evaluation with the TNM stage of tumor together with the other factors like renal function, comorbidities, and performance status, dictates the type of nephrectomy to be performed such as partial nephrectomy (excision of tumor part only) or radical nephrectomy (excision of whole kidney). Other therapeutic approaches can also be applied including embolisation and minimal invasive techniques (radiofrequency ablation, cryoablation, microwave ablation, laser ablation, and high intensity focused ultrasound ablation) to older patients or the patients who have high risk for surgery [14].

In metastatic RCC, the chemotherapy is not generally recommended due to the low response rate. Furthermore, the use of interleukin-2 and interferon in immunotherapy are under debate because of the high toxicity. However, immunotherapy might be helpful in some RCC patients and show more effectiveness than chemotherapy [11]. In targeting therapy, the targeting agents are used to inhibit the signaling pathways stimulating angiogenesis and cell growth. Especially, Sunitinib (receptor tyrosine kinase inhibitor) is used in treatment of metastatic RCC. Additionally, Sorafenib (VEGF receptor and Raf inhibitor), Bevacizumab (monoclonal antibody, VEGF blocker), Pazopanib (receptor tyrosine kinase inhibitor), Temsirolimus (inhibitor of mTOR, the protein that involves the regulation of cell growth and survival) and Everolimus (mTOR inhibitor) are utilized in the treatment of metastatic RCC. Emerging results suggested that these targeting agents increase the survival rate and give more promising outcomes compared to the chemotherapeutic and immunotherapeutic agents [16].

1.4. TISSUE TRANSGLUTAMINASE

1.4.1. Transglutaminases

Transglutaminases are a protein family of enzymes that perform the post-translational modifications of proteins [17]. Members of transglutaminase protein family cross-link proteins through an acyl-transfer reaction between ε-amino group of lysine residue and γ-carboxamide group of glutamine residue of the proteins to form an isopeptide bond (ε-(γ-glutamyl)lysine isopeptide bond) which is resistant to mechanical and proteolytic degradation [18, 19]. This transamidating activity is in Ca^{2+} dependent manner [20] which stimulates a conformational change at the structure of the enzyme protein. As result of the reaction, ammonia is released and covalently linked proteins are formed [21].

Primary amines and polyamines can also serve as substrate for transglutaminases in amine incorporation reactions. They catalyze the formation of (γ–glutamyl)-polyamine bond between a polypeptide-bound glutamine and the polyamine via incorporating the amine into the glutamine residue of the proteins [22, 23].

It was reported that transglutaminases can also achieve the hydrolysis of amides via the removal of amide group from glutamine residue of proteins [24] and, moreover transglutaminases (tissue transglutaminase and FactorXIIIa) were shown to posses isopeptidase activity and can hydrolyse ε-(γ-glutamyl)lysine isopeptide bond [25].

1.4.2. Tissue transglutaminase as a versatile protein

Tissue transglutaminase (TG2) is a member of enzyme family of transglutaminases. Different from other partners it is widely expressed in different types of cells and tissues [26].

In addition to Ca^{2+} dependent crosslinking activity of TG2 as stated above, it was reported that TG2 has guanosine triphosphate (GTP) binding site and exhibits magnesium dependent GTPase activity. Similarly, adenosine triphosphate (ATP) was also reported to

be hydrolysed by TG2 in a magnesium dependent manner [27, 28]. A previous study also showed that TG2 activity is inhibited by non-competitive binding of guanosine nucleotide suggesting that the crosslinking activity of the enzyme is regulated by the function of GTP and Ca^{2+} [29]. Following studies were also showed that Mg-ATP and Mg-GTP complexes induce different conformational changes in TG2. Mg-ATP binding inhibits GTPase activity of TG2 but not calcium-dependent transglutaminase activity whereas Mg-GTP binding inhibits calcium-dependent transglutaminase activity but not ATPase activity [28] Evaluating of these results suggests that TG2 activity is modulated by the concentrations of Mg-ATP, Mg -GTP complexes together with Ca^{2+} concentration in cellular milieu where TG2 resides.

TG2 is also suggested to exhibit protein disulphide isomerase (PDI) activity and converts denaturated inactive Rnase A molecule to the native active form via establishing disulphide bonds at certain sites of polypeptides. Furthermore, it was also declared that the PDI activity is catalysed by a domain of TG2 different from its transamidating and GTPase activity domains because the PDI activity neither required Ca^{2+} nor affected by the presence of nucleotides [30].

Recent studies indicated that TG2 also shows an intrinsic kinase activity. First evidence for kinase activity was shown in human breast cancer cells that TG2 phosphorylates insulin-like growth factor-binding protein-3 [31]. Another study about the kinase activity of TG2 also showed that TG2 can phosphorylate p53. Since TG2 phosphorylation sites of p53 are important in p53 degradation, the kinase activity of TG2 on p53 might assist the accumulation of p53 and thereby facilitate the apoptosis [32]. In a recent study it was shown that TG2 has the ability to phosphorylate retinoblastoma protein and also its kinase activity is enhanced via the phosphorylation of TG2 by protein kinase A [33]. All three studies together indicated that the kinase activity of TG2 is inhibited by Ca^{2+} concentration.

1.4.3. TG2 Activity

TG2 can be located in the different parts of cells including nucleus, cytosol, mitochondria, cell surface and the extracellular matrix (ECM) (Figure 1.4) [34]. In normal

physiological state the activity of TG2 in these compartments is closely controlled by the presence of Ca^{2+} and nucleotides (GTP/GDP and ATP/ADP), and inside the cell under low Ca^{2+} concentration and high concentration of GTP/ATP TG2 cross-linking activity remains in latent status [35]. However, in ECM where Ca^{2+} concentration is high and GTP/GDP and ATP/ADP concentration is low, TG2 can actively crosslink the proteins and increase the matrix stability. It was revealed that TG2 activates a cytokine, transforming growth factor-β (TGF-β) via inducing the dissociation of latent TGF-β binding protein from inactive TGF-β complex [36]. As TGF-β increases, ECM deposition stimulating the synthesis of ECM proteins like collagen, FN [37, 38] and tissue inhibitors of metalloproteinases (TIMP) while decreasing transcription of the matrix metalloproteinases (MMP), which are endopeptidases capable of degrading the ECM proteins. Therefore, by activation of TGFβ1, TG2 increase the biosynthesis of ECM proteins [39, 40].

Independent from crosslinking activity TG2 can also act as a signaling molecule in cell adhesion and cell survival via interacting with β1 and β3 integrins (cell attachment receptors) and syndecan-4 (heparan sulfate proteoglycan) on the cell surface [41, 42].

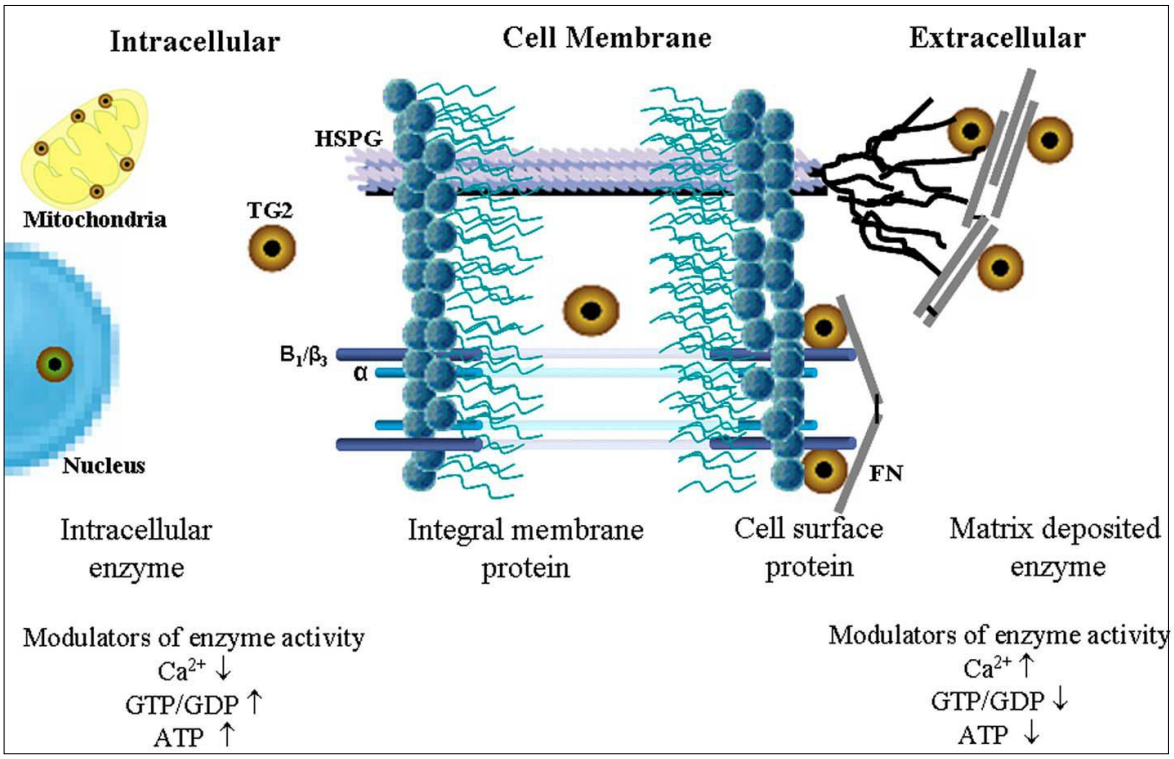

Figure 1.4. Cellular localization of TG2 [43]

TG2 is involved in cell adhesion by binding to fibronectin (FN) which is one of the extracellular substrates of TG2. After deposition of TG2 into ECM, TG2 binds to FN and forms a complex that can associate with the heparan sulfate proteogylcans syndecan-4 and induce the cell adhesion [43].

FN is a glycoprotein that constitutes the main component of extracellular matrix. It is involved in various adhesive and migratory events related with different physiological processes such as tissue repair, neovascularization and embryogenesis [44]. Functional form of FN is the multimeric fibrillar form which is found in ECM. The cells produce and deposit FN in ECM through a process which is tightly controlled and contains multiple steps to build an appropriate matrix [45]. FN binds to cells via the interaction with cell surface integrin proteins. FN binds to α5β1and αIIBβ3 integrins through its Arg-Gly-Asp (RGD) containing cell adhesion site [46]. Integrin mediated cell adhesion to FN elicits the formation of integrin clusters and integrins clustering at sites of matrix contact triggers the assembly of cell-matrix junctions called focal adhesions. Focal adhesions are multiprotein complexes that include the accumulation of multiple cytoskeletal and signaling molecules around the integrin cytoplasmic domain [47]. Focal adhesions are linked to actin/myosin filaments (stress fibers) inside the cells and activate signaling pathways inside the cell [48]. Among many of the proteins, cytoplasmic tyrosine kinase called focal adhesion kinase (FAK) interact with integrins at focal adhesions and activates signaling pathways, such as mitogen-activated protein kinase, protein kinase C, and phosphatidylinositol 3-kinase pathways [49].

Integrins are cell surface receptors mediating cell adhesion to ECM proteins and cell-cell adhesions. Besides the role in cell adhesion, integrins connect with cytoskeleton and activates the intracellular signaling pathways which have key roles in the development, immune responses, leukocyte traffic, hemostasis, and cancer [50]. The integrins are heterodimeric proteins which are composed of α and β subunits. In mammals, 19 α and 8 β subunit genes encoding polypeptides has been detected and these proteins form 25 different receptor combinations [51].

Integrins can bind to a variety of extracellular ligands including fibronectin, collagen, laminin, vitronectin, and fibrinogen. The integrin-ligand interaction requires the

binding of bivalent cations to integrins which results in a conformational change in the integrin molecule and exposure of the ligand-binding sites within integrins [52, 53, 54]. Integrins are generally inactive state on the cell surface in that they do not bind to their ligands. Activation and ligand binding of integrins are regulated by the interactions between the cytoplasmic domain of integrin and intracellular proteins. The cells regulate integrin mediated adhesion via changing the integrin affinity for ligands. This process is called as ‘‘inside-out’’ signaling [55]. However, ligand binding to integrins leads to the transduction of signals into the cell resulting in the cytoskeletal re-organization, gene expression and cellular differentiation. This process is called as ‘‘outside-in’’ signaling [56]. The cytoplasmic domains of integrins are the key elements in these bi-directional signaling [57]. Integrins clustering at the focal adhesion sites provide a structural link between the actin cytoskeleton and the extracellular matrix. The aggregation of integrins activates the focal adhesion kinase and leads to the assembly of complex structure containing a number of proteins that are involved in the signal transduction [48].

Syndecans are a family of transmembrane heparan sulfate proteogylcans that participate in some important biological organization such as cell adhesion, growth-factor signaling, lipase activity and anticoagulation [58]. Syndecan molecules have an extracellular domain which is modified with attachment of heparan sulfate chains, a characteristic transmembrane region and a conserved short C-terminal cytoplasmic domain [59]. Syndecan-4 is ubiquitously expressed member of syndecan family in cells from different origin. In cell adhesion, syndecan-4 behaves as co-receptor for integrins since the extracellular-matrix proteins recognize the heparan sulfate chains of syndecan-4 [60]. Additionally, syndecan-4 was shown as accessory signaling molecule modulating integrin-based adhesion since it was demonstrated that syndecan-4 can directly bind to FN and contribute to the generation of stress fibers and focal adhesions together with α5β1 integrin via the activation of protein kinase C α (PKCα) and Rho [61].

TG2 associates with FN in ECM and TG2-FN complex interacts with β1 and β3 integrins on the cell surface. Integrin mediated adhesion to FN enhances in the presence of TG2. Thus, integrins can interact with FN indirectly via binding to TG2 in complex with FN as well as their direct interaction [41]. In addition to this, TG2 maintains cell adhesion in response to RGD inhibitory peptides occurring following the degradation of ECM by

matrix metalloproteinases. In this RGD-independent cell adhesion pathway, FN bound TG2 complex interacts with SDC4 and activated SDC4 stimulates PKCα which is a downstream signaling molecule of SDC4. Then PKCα initiates the inside-out activation of integrins. Integrin activation leads to actin stress fiber organization and the activation of FAK and ERK1/2 hence promote the cell survival [42].

As a result of different locations and interactions with various molecules, TG2 can be involved in several physiological processes such as tissue fibrosis, wound healing, apoptosis, neurodegenerative disorders, celiac disease, atherosclerosis and cancer.

1.4.4. TG2 in Cancer

It is not clear whether TG2 has an inhibitor or activator role in the tumor progression. Cytosolic TG2 might behave as pro-apoptotic [62, 63] or anti-apaoptotic [64] factor depending on the cellular context. TG2 may be involved in insensitivity to growth signals and resistance to apoptosis in tumor cells with its GTP binding and transamidating properties [65]. Transfection of active and inactive form of TG2 into malignant hamster fibrosarcoma showed that both forms of TG2 might cause a delay in the progression of cell cycle from S-phase to G2/M suggesting that GTP binding activity of the TG2 and not crosslinking activity is the reason of its effect [66]. TG2 may also contribute to apoptosis mediating the transamidation of retinoblastoma protein and posttranslationally modified retinoblastoma protein might behave as a key signal for the initiation of apoptosis [67]. On the contrary, intracellular TG2 can contribute to the inhibition of apoptosis through activating the transcription factor nuclear factor-κB in breast and pancreatic cancer cells [68].

Cancer is a multistep process that initiates in primary tumor and occurrence of a series of events cause the tumor progression and metastatic tumors. The main biological processes including cell adhesion, migration, ECM homeostasis, and angiogenesis are important in the tumor formation and progression. Cells in tissues reside in ECM attaching to ECM components or one another cell. ECM attachment involves in basic biological processes of cells such as normal growth, differentiation, and function. Disruption of

adhesion to ECM leads to disruption in cell proliferation in tumor formation and invasive properties, and metastatic potential in tumor progression [69, 70].

In the extracellular environment, TG2 involves in cell adhesion and cell survival as explained above. TG2 maintains cell adhesion by acting as integrin-binding adhesion co receptor for FN [41] and also in RGD-independent cell adhesion pathway by activating syndecan-4 and integrins which trigger the survival kinase pathway [42]. TG2 expression might be reduced in early stages of tumor formation (in primary tumors) but its expression increases with the metastasis and confers drug resistance to the tumor [71]. Elevated expression level of TG2 in tumor cells has been reported in various studies and this increase is generally associated with the metastatic potential and drug resistance of tumor cells. For instance up-regulated TG2 expression was shown in the metastatic breast cancer cells exhibiting drug resistance [72]. Moreover, the expression of TG2 in breast cancer cells and also malignant melanoma cells can contribute to the metastatic phenotype and drug resistance through increasing the cell attachment and cell survival provided by the interaction of FN bound TG2 with integrins on the cell surface [73, 74, 75]. Another study has revealed FAK colocalization with TG2 at focal adhesion is prevalent in the pancreatic ductal adenocarcinoma [76].

On the other hand, following the overexpression of membrane type 1-matrix metalloproteinase proteolytic degradation of TG2 inhibits cell adhesion and movement of tumor cells on FN while FN protects TG2 from proteolytic degradation. This mechanism might also be thought as a regulatory mechanism of tumor cells in relation to their metastatic behavior [77].

Angiogenesis, formation of new blood vessels, is another important and essential mechanism in tumor progression and metastasis. A study showed that TG2 expression is down regulated in time during the human capillary morphogenesis suggesting that low TG2 is desired in the initial steps of the angiogenesis [78]. Supporting these findings, TG2 increase can inhibit endothelial tube formation during angiogenesis and generates cross-linked ECM proteins without leading cell death. Likewise, administration of catalytically active TG2 into mice with CT26 colon carcinoma tumor decreases the vessel organization

and at the same time increases the formation of fibrotic-like tissue and ε-(γ-glutamyl) lysine bonds and therefore provides a reduction in tumor growth [79].

1.4.5. Aim of the Study

The aim of the study is to investigate the importance of TG2 in the kidney cancer. In the early studies, decreased TG2 expression and activity was reported in primary tumors suggesting tumor cells want to generate more destabilized ECM for tumor growth [72, 75] while increased TG2 expression in association with increased integrin β1 expression correlates with metastasis and drug resistance in tumor cells [73, 74]. On the cell surface TG2 may not show its enzymatic activity, however, it can induce cell survival when interact with syndecan-4 and associate with integrin β1 on cell surface [41, 42].

In the light of previous data, in this study expression of TG2 along syndecan-4 and integrin β1 was investigated in primary tumors and their healthy counterparts taken from RCC patients. Total RNA was isolated from tissues and tested for expression experiments. As *in vitro* model, Caki-2 and A-498 cell lines isolated from primary RCC tumors were selected along with the control cell line RPTEC which was isolated from healthy kidney. For the assessment of TG2 activity in RCC primary tumors, healthy tissues together with Caki-2, A-498 cancer cell lines and RPTEC control cell line, TG2 activity assay was also performed.

2. MATERIALS

2.1. INSTRUMENTS

The instruments used in this study are as follows:

- Laminar flow cabinet (ESCO Labculture Class II Biohazard Safety Cabinet Type 2A, Singapore)
- CO_2 incubator (Nuaire NU5510/E/G, USA)
- Inverted phase contrast microscope (Nikon Eclipse TS-100, USA)
- Centrifuge (Hettich mikro 22R, Germany and SİGMA 2-5 centrifuge, Germany)
- Vortex (Stuart SA8, UK)
- pH meter (Hanna instruments PH211, Germany)
- Spectrophotometer (Implen Nanophotometer, USA)
- PCR Thermal Cycler (Biorad MyCycler, USA)
- Real-time PCR Thermal Cycler (Biorad iCycler iQ multicolor detection system, USA)
- Mini-PROTEAN Tetra Cell Electrophoresis System (Bio-Rad 165-8001, USA)
- Mini Trans-Blot Cell Blotting System (Bio-Rad 170-3935, USA)
- Chemiluminescence imaging system (DNR Systems MF-ChemiBIS 3.2, Israel)
- -80 °C freezer (Thermo Forma -86C ULT Freezer, USA)
- Homogenizator (Pellet pestles Sigma Z359947 and Cordless motor Sigma Z359971, USA)
- ELISA plate reader (Bio-Tek Elx800, USA)

2.2. EQUIPMENTS

The laboratory equipments used in this study are as follows:

- Cell culture flasks, T-25, T-75, T-150 and cell culture plates, 6-well, 96-well, (TPP, Switzerland or Grenier-Bio, Germany)

- Cryovials (TPP, Switzerland)
- Micro pipettes 1000, 200, 100, 10, 2.5 µl (Thermo Scientific, USA)
- Polypropylene centrifuge tubes, 50 ml, 15 ml, 2 ml, 1 ml, 0.5 ml (Isolab, Germany)
- Serological pipettes 25, 10, 5, 2 ml (Lp Italiana Spa, Italy or Axygen, USA)

2.3. CHEMICALS

The chemicals used in this study are as follows:

- Cell culture media:
  - Dulbecco's Modified Eagle's Medium – high glucose (Sigma D6429 or Gibco 41966, USA)
  - McCoy's 5A Medium (Thermo Scientific SH 30200.01, USA or PAN Biotech P04-00501, Germany)
  - Renal Epithelial Cell Basal Medium (ATCC Primary Cell Solutions PCS-400-030, USA)
- Growth supplements:
  - Fetal Bovine Serum (FBS) – Cell culture tested (Sigma F9665)
  - Non-essential amino acid (Sigma M7145)
  - Renal Epithelial Cell Growth Kit (ATCC Primary Cell Solutions PCS-400-040, USA)
- 2-Mercaptoethanol (Merck 805740, Germany)
- 2-propanol (AppliChem A3928, Germany)
- 3,3′,5,5′-Tetramethylbenzidine (TMB) (Sigma T2885,China)
- Absolute Ethanol (AppliChem A3678, Germany)
- Acrylamide/Bis-acrylamide (29:1) (Sigma A3574, USA)
- Ammonium persulfate (Sigma A3678, USA)
- Biotin cadaverine, trifluoroacetate salt (N-(5-aminopentyl) biotinamide, trifluoroacetic acid salt) (Biotium 90063, USA)
- Bovine serum albumin (Sigma A7030, USA)
- $CaCl_2$ (Riedel-de Haen 12022, Germany)
- Casein from bovine milk (Fluka 22080, Germany)

- Chloroform (Aldrich 528730, USA)
- Dimethyl sulfoxide (Santa Cruz sc-202581, USA)
- Dithiothreitol (DTT) (AppliChem A1101, Germany)
- Dulbecco's Phosphate Buffered Saline (DPBS) (PAN Biotech P04-53500, Germany)
- Ethylenediaminetetraacetic acid (EDTA) (Merck 108418, Germany)
- Fibronectin from human plasma (Sigma F0895, USA)
- Glycine for electrophoresis (Merck 104169, Germany)
- H_2SO_4 (Riedel-de Haen 07208, Germany)
- L-Glutamine (Invitrogen 25030, USA)
- Methanol 99% (Sigma 34885, USA)
- N,N,N′,N′-Tetramethylethylenediamine (TEMED) (Sigma T7024, China)
- Penicillin-streptomycin (Thermo Scientific SV30010, USA or Biochrom A2213, Germany)
- Phosphate-Citrate Buffer with Urea Hydrogen Peroxide (Sigma P4560, USA)
- Sodium deoxycholate (Sigma D6750, New Zeland)
- Sodium dodecyl sulfate (Merck 822050, Germany)
- Tris-base (Merck 108387, Germany)
- Tris-HCl (Merck 108219, Germany)
- Trizol (Invitrogen 15596-018, USA)
- Trypsin-EDTA (Biochrom L2153, Germany)
- Tween-20 (Merck 822184, Germany)

2.4. KITS AND SOLUTIONS

The commercially available kits that were used in this study were as follows:

- Amersham ECL Advance Western Blotting Detection Kit (GE Healthcare RPN2135, USA)
- Amersham Hybond-ECL Nitrocellulose Membrane (GE Healthcare RPN303D, USA)
- Amersham Rainbow protein marker (GE Healthcare RPN 800E, USA)
- Bovine serum albumin, protein standard (Sigma P0834, USA)

- Cell Proliferation Reagent WST-1 (Roche 05015944001, Germany)
- Comassie Protein Assay Kit (Pierce, 23200, USA)
- Extravidin peroxidase (Sigma E2886, Israel)
- Oligo dT primer (Qiagen 79237, Germany)
- QuantiTect Primer Assay for TGM2 (Qiagen QT01009519, Germany)
- QuantiTect Primer Assay ITGB1 (Qiagen QT00068124, Germany)
- QuantiTect Primer Assay RRN18S (Qiagen QT00199367, Germany)
- QuantiTect Primer Assay SDC4 (Qiagen QT01008126, Germany)
- QuantiTect SYBR Green PCR Kit (Qiagen 204145, Germany)
- RIPA Lysis Buffer (Santa Cruz sc-24948, USA)
- Sensiscript RT Kit (Qiagen 205213, Germany)

2.5. ANTIBODIES

2.5.1. Primary Antibodies

- Integrin β1 antibody (Santa Cruz, sc-8978, USA)
- Syndecan-4 antibody (Zymed 36-3100, USA)
- TG2 antibody (Thermo Scientific, Labvision Cub 7402, MS-224-P, USA)
- β-actin antibody (Santa Cruz sc-81178, USA)

2.5.2. Secondary Antibodies

- Anti-mouse IgG peroxidase conjugate (Sigma A4416, USA)
- Anti-rabbit IgG peroxidase conjugate (Sigma A0545, Israel)

2.6. HUMAN TISSUE SAMPLES AND CELL LINES

2.6.1. Tissue Sample Collection

Kidney tumor and healthy tissues were collected from 61 patients that were previously diagnosed with RCC at Department of Urology, Istanbul Faculty of Medicine,

Istanbul University. During the radical nephrectomy operation of the patients, tissue specimens from center of the tumor and healthy part of the kidney were taken and washed with 0.9% (w/v) NaCl solution to clear the tissue samples from blood. Then, these tissue specimens were kept at -80°C and carried via cold chain transport. All patients were reported as RCC after histological evaluation. Histopathological evaluation and other features of patients are stated in Appendix section.

2.6.2. Cell Lines

All cell lines shown in Table 2.1 were obtained from American Type Culture Collection (ATCC).

Table 2.1. Cell lines that were used in the study

Cell Type	ATCC number	Growth Properties
Renal proximal tubule epithelial cells (RPTEC) from human kidney	PCS-400-010	Adherent
Caki-2, primary clear cell carcinoma of human kidney	HTB-47	Adherent
A-498, human kidney carcinoma	HTB-44	Adherent

RPTECs were used as control cell line and Caki-2, A-498 were used as the primary RCC cancer cell line model.

3. METHODS

3.1. RNA ISOLATION

3.1.1. RNA Isolation from Tissues

Total RNA extraction from tissues was performed using TRIzol (Invitrogen, USA) reagent. Tissue samples (50 mg) were homogenized with pellet pestle homogenizator in 1 ml TRIzol reagent. After a short spin to remove particles, supernatant was transferred to a new tube and 200 µl chloroform was added. The tubes were shaken vigorously and incubated for 10 minutes at room temperature. The tubes centrifuged at 12,000 x g for 15 minutes at 4°C. After centrifugation, the aqueous phase was transferred to a new tube and mixed with 500 µl isopropyl alcohol. The samples were incubated for 10 minutes at room temperature and centrifuged at 12,000 x g for 10 minutes at 4°C. Then supernatant was discarded, RNA pellet washed with 1 ml 75% ethanol and centrifuged at 7,500 x g for 10 minutes at 4°C. After the removal of supernatant RNA pellet was dried via vacuum-dry and dissolved in 50 µl Rnase-free water. RNA samples were stored at -80°C.

3.1.2. RNA Isolation from Cells

RPTECs (300.000 cells/well) were seeded on six-well plates per well and incubated for 48 hours. In order to presynchronize cancer cells at G_o by serum starvation Caki-2 and A-498 (300,000 cells/well) cells were seeded on 6-well plates per well and incubated for 48 hours in medium containing 2% (v/v) FBS. After incubation of cells, the medium was removed, cells were washed with 1xPBS and 500 µl TRIzol reagent was directly added to cell monolayer and scraped with pipette tip. After lysis of cells in TRIzol reagent by scrapping, samples were transferred a clean tube and 100 µl chloroform was added. The tubes were shaken vigorously and incubated for 10 minutes at room temperature. The tubes centrifuged at 12,000 x g for 15 minutes at 4°C. After centrifugation, the aqueous phase was transferred to a new tube and mixed with 250 µl isopropyl alcohol. The samples were incubated for 10 minutes at room temperature and centrifuged at 12,000 x g for 10 minutes at 4°C. Then, supernatant was discarded, RNA pellet was washed with 500 µl 75% ethanol

and centrifuged at 7,500 x g for 10 minutes at 4°C. After the removal of supernatant, RNA pellet was dried via vacuum-dry and dissolved in 50 µl Rnase-free water. RNA samples were stored at -80°C.

3.1.3. Quantification of RNA

The concentrations of isolated RNA samples were determined by using spectrophotometer (Implen Nanophotometer). Rnase-free water was used as blank and RNA samples were measured at 260 nm. RNA concentration was calculated from the absorbance at 260 nm using equation below:

''Concentration of RNA sample (ng/µl) = 40 x A_{260} x dilution factor'' (Equation 3.1)

As proteins give absorbance at 280 nm, the protein contamination in RNA samples was measured by calculating the A_{260}/A_{280} ratio.

3.2. POLYMERASE CHAIN REACTION

3.2.1. Reverse Transcriptase Polymerase Chain Reaction

Reverse transcriptase polymerase chain reaction (RT-PCR) for synthesis of complementary DNA (cDNA) Qiagen Sensiscript RT Kit was used. After quantification of RNA sample, 1000 ng template RNA was transferred to a new tube in 13 µl Rnase-free water. Then, 7 µl reaction mixture that contains 2 µl 10x Buffer RT, 2 µl dNTP Mix (5 mM each dNTP), 2 µl Oligo-dT primer (10 µM), 1 µl Sensiscript Reverse Transcriptase was added to the tube and 20 µl total volume was obtained. The samples were then incubated at 37°C for 60 minutes. After incubation, reaction mixture was diluted (4 fold) and samples were stored at -20°C.

3.2.2. Quantitative Real-Time Polymerase Chain Reaction

The mRNA expression levels of TG2, syndecan-4 and integrin β1 genes in the tissue samples and cell lines were determined using QuantiTect SYBR Green PCR Kit in Bio-

Rad iCycler iQ5 instrument. Each reaction containing 6.25 µl SYBR Green PCR master mix, 1.25 µl primer mix (QuantiTect Primer Assays, TGM2, SDC4, ITGB1, 18SrRNA as internal control) and 500 ng cDNA (2 µl) in a total volume of 12.5 µl was performed in conditions given in the Table 3.1.

Table 3.1. Real-time PCR conditions

Cycle	**Temperature**	**Time**	**Phase**
1	94°C	15 min	
2	95°C	5 min	Initial denaturation
3 (40 repeat)	95°C	60 sec	Denaturation
	55°C	60 sec	Annealing
	72°C	60 sec	Extension
4	72°C	10 min	Final extension
5 (80 repeat)	50-80°C 0.5 °C increase /12 sec		Melt curve
6	4°C	∞	Cooling

Figure 3.1 represents the PCR amplification/cycle graph or real-time PCR analysis. The specificity of PCR products were checked by melt curve analysis which was shown in Figure 3.2 (as an example of one of the PCR results). Each sample was studied in duplicate. The quantification of results was done by using standard curve method in which normalization of TG2, syndecan-4 and integrin β1 expressions was performed against the 18SrRNA expression values. Figure 3.3 also shows a standard curve graph to the one of PCR analysis.

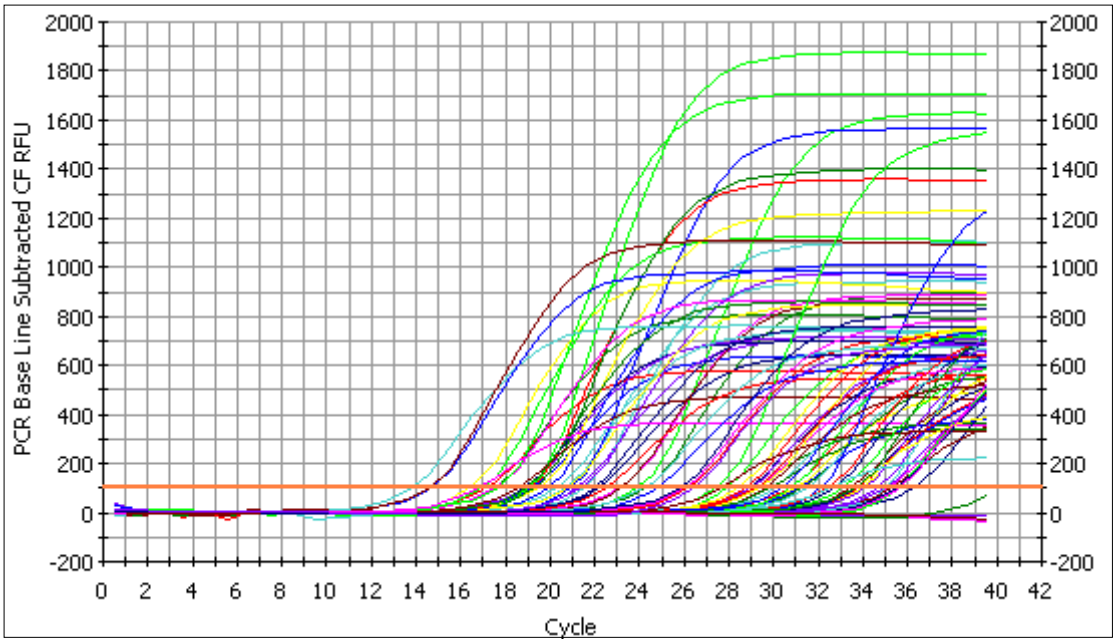

Figure 3.1. PCR amplification/cycle graph of one of the PCR results

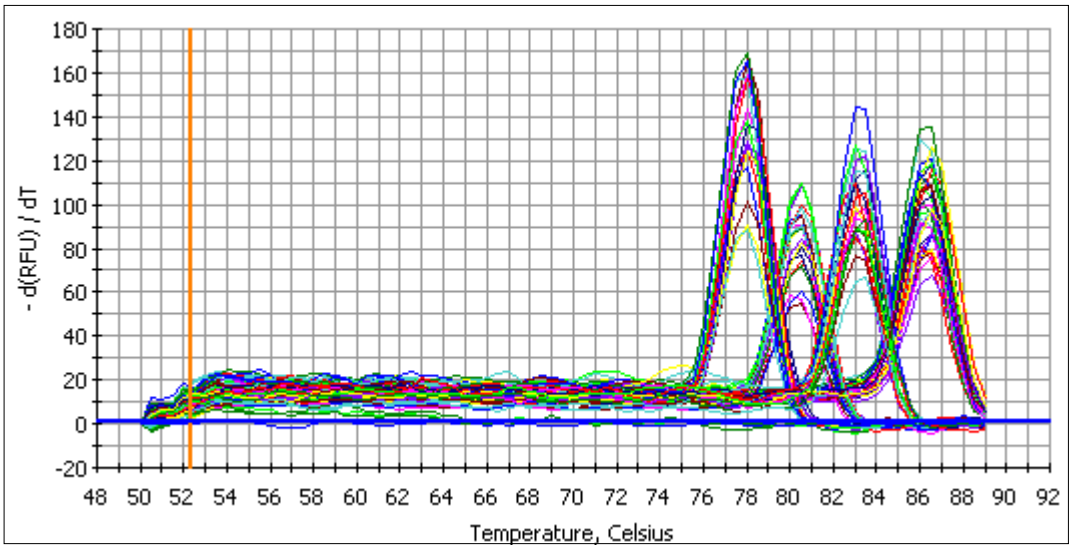

Figure 3.2. Melt curve analysis of one of the PCR results

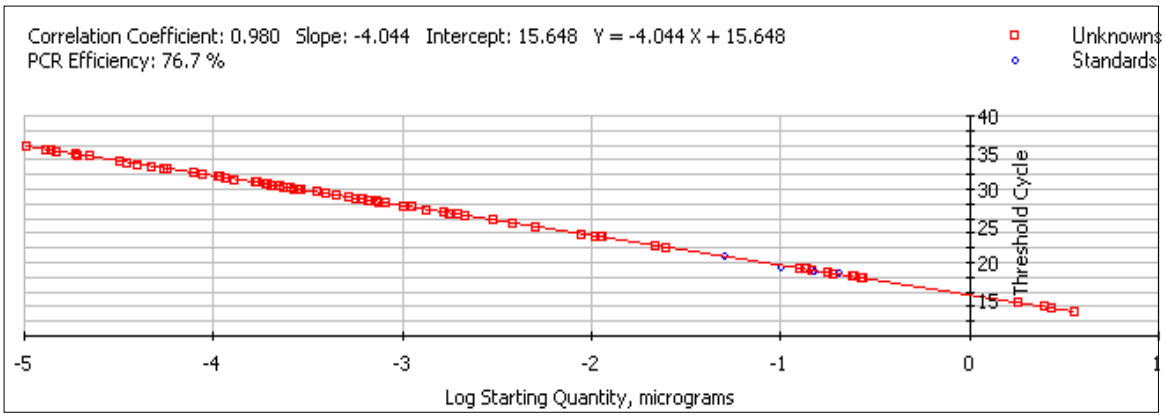

Figure 3.3. Standard curve of one of the PCR results

3.3. CELL CULTURE METHODS

3.3.1. Cells and Culture Conditions

For cultivation of RPTECs, Renal Epithelial Cell Basal Medium and Renal Epithelial Cell Growth Kit were purchased from ATCC. RPTECs were grown in basal media supplemented with growth kit including 10 nM triiodothyronine, 10 ng/ml epidermal growth factor, 100 ng/ml hydrocortisone hemisuccinate, 5 µg/ml insulin, 1 µM epinephrine, 5 µg/ml transferin, and 0.5% (v/v) Fetal bovine serum (FBS) and additionally 50 units/ml penicillin, 50 µg/ml streptomycin at 37 °C with 5% CO_2 atmosphere.

Caki-2 cancer cells were maintained in McCoy's 5A Modified media supplemented with 10% (v/v) FBS, 2 mM L-glutamine, 100 units/ml penicillin, 100 µg/ml streptomycin, 0.1 mM MEM Non-essential Amino Acid Solution at 37 °C with 5% CO_2 atmosphere.

A-498 cancer cells were also grown in Dulbecco's Modified Eagle Medium (DMEM) supplemented with 10% (v/v) FBS, 2 mM L-glutamine, 100 units/ml penicillin, 100 µg/ml streptomycin, 0,1 mM MEM Non-essential Amino Acid Solution at 37°C with 5% CO_2 environment.

3.3.2. Cell Passaging

After removal of media, cells were washed once with DPBS solution containing 137 mM NaCl, 2.7 mM KCl, 10 mM sodium phosphate dibasic, 2 mM potassium phosphate, pH 7.4. The cells were detached with adding 1 volume of trypsin (0.5 g/l)-EDTA (0.2 g/l) solution (1 ml for T-25 flasks, 2.5 ml for T-75 flasks) and incubating the flask for 3-5 minutes at 37°C with 5% CO_2 humidified incubator. The detached cells were collected in a centrifuge tube and 2 volumes of 10% (v/v) FBS supplemented medium was added to neutralize trypsin. After centrifugation of the mixture at 300 x g for 5 minutes, the supernatant was discarded and the cell pellet was resuspended in growth media to be seeded cells in a new flask.

3.3.3. Cell Counting

Cell counting was performed using the hemocytometer. Following cell detachment, 10 µl of cell solution was added to hemocytometer. The cells were counted using inverted phase contrast microscope (Nikon, USA). The circled area on the hemocytometer represents 1/10000 of 1ml (Figure 3.1).

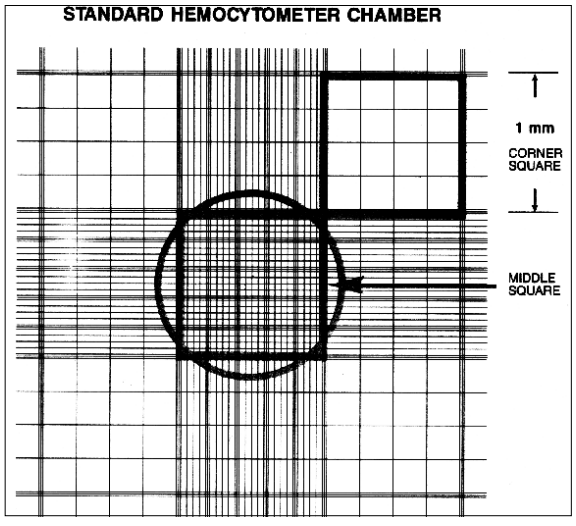

Figure 3.4. Hemocytometer chamber [80]

The cells on this square were counted for 4 different times and then average of these numbers was used to calculate the number of cells per ml using the formula:

''Cells/ml = the average number x 10^4 x dilution factor'' (Equation 3.2)

3.3.4. Cell Freezing

After trypsinization and cell counting, cell suspension was centrifuged at 300 x g for 5 minutes, supernatant was removed and cell pellet was resuspended in freezing media that contains 90% (v/v) FBS, 10% (v/v) dimethylsulfoxide (DMSO) at a concentration of $1x10^6$ cells/ml. Cells dissolved in freezing media was placed in cryovials to be transferred to -80°C for short term storage. For long-term storage, the cells were transferred to liquid nitrogen from -80°C freezer.

3.3.5. Cell Thawing

The frozen cell vial was taken from -80°C freezer or liquid nitrogen and was rapidly thawed at 37°C. Cell solution was transferred to a centrifuge tube and 5 ml of supplemented media was added slowly with gentle shaking. The tube was centrifuged at 300 x g for 5 minutes and the supernatant was discarded. The cell pellet was resuspended in growth media and cells were seeded on T-25 flask. The following day, culture media was removed; cells were washed with PBS, pH 7.4 and fresh media was added.

3.3.6. Serum Starvation and Cell Proliferation Assay

Before RNA isolation and cell lysis, synchronization of the cells was achieved through the serum starvation of cells. Serum starvation arrests the cell cycle at G_0/G_1 phase and different cells showing different doubling time become synchronized. To determine the optimum serum concentration for cell starvation, different serum concentrations were studied ranging from 1 to 10% (v/v) FBS. Cell proliferation rate was determined with Cell Proliferation Reagent WST-1 (Roche, Germany). Cells were seeded in triplicate on 96-well plates at a density of 5000 cells/well in 100 µl culture media supplemented with assigned FBS concentrations and incubated for 48 hours. Then, the media was removed and 50 µl

fresh media and 5 µl WST-1 reagent were added to each well and the plate was incubated at 37°C for 1 hour. The absorbance of each sample was measured at 450 nm with 630 nm reference wavelength in ELISA plate reader (Bio-Tek, USA).

WST-1 tetrazolium salt is cleaved to formazan by mitochondrial enzymes. Activity of mitochondrial dehydrogenases in cells increases as the number of cells increases. Therefore the increase in the formazan formation is directly correlated with the number of metabolically active cells. Via the quantification of formazan dye by spectrophotometer, the cell proliferation is measured.

3.4. MEASUREMENT OF TG2 ACTIVITY

3.4.1. Measurement of TG2 Activity via Biotin Cadaverin Incorporation in Tissue Samples

Tissue samples were homogenized in 300 µl 1% (w/v) sodium deoxycholate solution. After removal of tissue particles with short spin centrifuge tissue lysate was transferred to a new tube and sonicated for 15 minutes in a sonicator bath at 4^{o}C. Protein content of samples was determined by Bradford assay as described in section 3.5.2. Protein sample (15 µg) in 50 µl final volume was prepared by diluting with 1% (w/v) sodium deoxycholate. 96-well plate coated with 250 µl of 10 mg/ml casein in 0.1 M Tris-HCl, pH 8.5 for 16 hours at 4°C was washed twice with PBS, pH 7.4 and once with 0.1 M Tris-HCl, pH 8.5 for 5 minutes on gentle shaking. Reaction mixture (150 µl) that contains 13.3 mM DTT, 6.67 mM $CaCl_2$, 0.1 mg/ml biotin cadaverin (BTC) in 0.1 M Tris-HCl and 50 µl protein sample was added to each well. The plate was incubated for 2 hours at 37 °C. After incubation, the wells were washed three times with 0.1 M Tris-HCl, pH 8.5 for 5 minutes with gentle shaking. In order to label casein incorporated BTC, extravidin peroxidase diluted 1:1000 in 0.1 M Tris-HCl, pH 8.5 containing 1% (w/v) BSA was added to each well (200 µl/well) and incubated for 45 minutes at 37°C. The wells were washed three times with 0.1 M Tris-HCl, pH 8.5 and equilibrated with the developing buffer containing 0.1 M NaOAc, pH 6. Reaction was developed by addition of 200 µl developing buffer containing 75 µg/ml 3,3',5,5'-Tetramethyl benzidine (TMB), the substrate for the peroxidase (dissolved in DMSO). After formation of the blue color, the reaction was

terminated by addition of 50 µl of 2.5 M H_2SO_4 and absorbance was measured at 450 nm in ELISA plate reader (Bio-Tek, USA).

3.4.2 Measurement of Cell Surface TG2 Activity via Biotin Cadaverin Incorporation

96-well plate were coated with 5 µg/ml FN in 50 µM Tris-HCl, pH 7.4 for 16 hours at 4°C or 1 hour at 37°C and blocked with 3% (w/v) BSA in PBS, pH 7.4 for 30 minutes at 37°C. The plate was gently washed three times with 50 µM Tris-HCl, pH 7.4 for 5 minutes on a shaker. Serum starved RPTEC, Caki-2, and A-498 cells were trypsinized and resuspended in serum free media. The cells were counted and seeded on FN coated plates at 20000 cells/well density in serum free media containing 0.132 mM BTC and incubated for 2 hours at 37°C. For negative background control, FN coated wells were incubated with serum free media containing 0.132 mM BTC. After incubation, the wells were washed twice with PBS, pH 7.4 and 100 µl of 0.1 % (w/v) sodium deoxycholate was added to each well followed by gentle shaking for 10 minutes. Following three-5 minute washes with 50 µM Tris-HCl, pH 7.4, 100 µl of extravidin peroxidase (dissolved 1:1000 in 0.1 M Tris-HCl, pH 7.4 containing 3% (w/v) BSA was added to each well to reveal incorporated BTC and incubated for 1 hour at 37°C. After three-5 minutes washes with µM Tris-HCl, pH 7.4 and a single wash with the developing buffer 0.1 M NaOAc, pH 6, the reaction was developed as described before by addition of 100 µl of developing buffer containing TMB to each well. By the addition of 50 µl of 2.5 M H_2SO_4 to each well, the reaction was terminated and absorbance was measured at 450 nm using an ELISA plate reader (Bio-Tek, USA).

3.5. MEASUREMENT OF TG2, SYNDECAN-4 AND INTEGRIN β1 PROTEIN LEVELS

3.5.1. Preparation of Total Cell Lysates

Whole cell lysate was obtained using RIPA lysis buffer (Santa Cruz Biotechnology, USA). Cells were seeded on 6-well plates and incubated in media containing 2% (v/v) FBS for serum starvation. After 48 hours, cells were washed once with DPBS, pH 7.4 and 30 µl complete RIPA buffer (contains protease inhibitor cocktail, PMSF, sodium orthovanadate

according to the manufacturer's data sheet) was added onto cell monolayers. Cells lysates were collected by a cell scraper in a new tube and sonicated on ice with a probe sonicator and stored at -80°C up to one month.

3.5.2. Bradford Assay

For determination of the protein content Pierce Comassie Protein Assay Kit-Microplate Procedure was used (Pierce, Thermo Scientific, USA). BSA standards were prepared by the serial dilution of 2 mg/ml BSA solution (Sigma, USA) at a working range of 0.1-1.5 mg/ml. To each well of a microtiter plate, 5 µl of each BSA solution and 1 µl unknown protein sample diluted in 4 µl dH_2O were added and incubated with 250 µl of Comassie reagent at room temperature for 10 minutes. The absorbance was measured at 590 nm using an ELISA plate reader (Bio-Tek, USA). The standard curve graph was prepared using absorbance values of BSA standard samples vs. their concentration to calculate the protein content of samples.

3.5.3. Sodium Dodecyl Sulfate Polyacrylamide Gel Electrophoresis (SDS-PAGE)

The stacking gel containing 4% (w/v) polyacrylamide and separating gels containing 8% or 10 % (w/v) polyacrylamide were used to separate proteins. The stacking gel and separating gels were prepared according to Table 3.2.

Table 3.2. The compositions of polyacrylamide gels with various percentages

	Final % (w/v) acrylamide concentration		
Stock solutions	4%	8%	10%
30% (w/v) acrylamide/ 0.8% bisacrylamide	0.65 ml	4 ml	5 ml
0.5 M Tris-HCl containing 0.4% (w/v) SDS, pH 6.8	1.25 ml	-	-
1.5 M Tris-HCl containing 0.4% (w/v) SDS, pH 8.8	-	3.75 ml	3.75 ml
dH_2O	3.05 ml	7.25 ml	6.25 ml
10% (w/v) APS	25 µl	50 µl	50 µl
TEMED	5 µl	10 µl	10 µl

SDS-PAGE was performed using Bio-Rad Mini-PROTEAN Tetra cell Electrophoresis System. The separating gel prepared according to Table 3.2 was immediately poured into the glass plates (80x60x1 mm) in the casting frame placed into the casting stand. 2-propanol was placed onto the gel to get a smooth gel surface. After polymerization of the gel at room temperature, 2-propanol was discarded and gel surface was washed with dH_2O. After removal of the excess water with the help of a filter paper, the stacking gel was prepared and added on to the separating gel. The 10-well comb was immediately placed into the stacking gel by avoiding air bubble formation and gel was left to polymerize at room temperature. After polymerization, the comb was carefully removed and the wells were washed with running buffer, pH 8.5 (25 mM Tris-Base, 192 mM glycine, 0.1% (w/v) SDS). Meanwhile, 30 µg protein samples mixed with 2x Laemmli Buffer (Sigma, USA) at 1:1 volume ratio boiled at 95°C for 5 minutes and cooled on ice. Protein samples and Amersham rainbow protein marker (GE healthcare, USA) were loaded to the wells carefully. Gel was then removed from the casting frame carefully and placed into U-shaped gasket and clamping frame, and inserted into the electrophoresis tank. Electrophoresis was carried out in running buffer pH 8.5 at 70V through the stacking gel for 15 minutes and 90V until the dye front reached to the bottom of the gel.

3.5.4. Western Blot

After the separation of proteins in the samples according to their molecular weight by SDS-PAGE, proteins on the gel were transferred to nitrocellulose membrane by Western Blot technique using Bio-Rad Mini Trans-Blot Cell System. Nitrocellulose membrane was cut according to gel size and equilibrated in cold transfer buffer, pH 8.3 (25 mM Tris-Base, 192 mM glycine and 20% (v/v) methanol) for 10 minutes. Sponge pads and filter papers were also soaked with cold transfer buffer, pH 8.3. Gel was carefully removed from the glass plates and washed with transfer buffer, pH 8.3. Gel sandwich was then prepared in gel holder cassettes as shown in Figure 3.2 by avoiding of the formation of air bubbles.

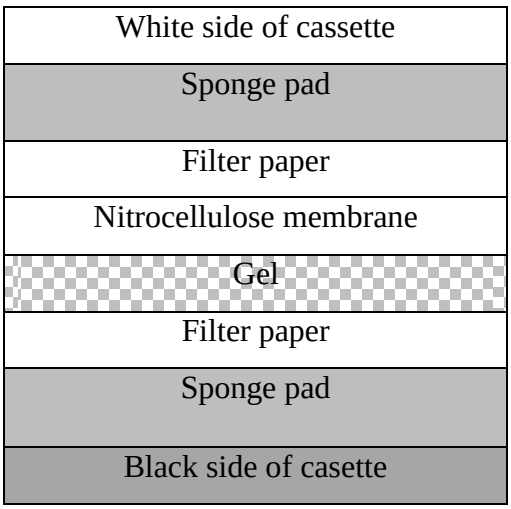

Figure 3.5. The assembly of transfer cassette for Western Blot

Cassette was then inserted into blotting apparatus by facing the gel side to the cathode electrode and the membrane side to the anode electrode. After the transfer of the apparatus into the tank contain cold transfer buffer, pH 8.3 and a cooling unit to prevent heating, the Western Blot transfer of the proteins was performed at 100 mA for 1.5 hours.

Transfer of proteins was confirmed by visualization of colored markers on the membrane. The membrane was washed once with TBS-Tween, pH 7.4 (100 mM Tris-HCl, 9% (w/v) NaCl, 0.5% (v/v) Tween 20) and blocked in 5% (w/v) non-fat dry milk in TBS-Tween, pH 7.4 for 1 hour with gentle shaking at room temperature. After blocking, the membrane was incubated with primary antibody against TG2, syndecan-4 or integrin β1.

1:5000 dilution was used for mouse monoclonal anti-TG2 antibody Cub7402 (LabVision, Thermo Scientific, USA), while 1:7500 dilution was used for rabbit polyclonal anti-syndecan-4 (Zymed Laboratories, Invitrogen, USA) and anti- integrin β1 (Santa Cruz Biotechnologies, USA) antibodies. The membrane was then washed twice with TBS-Tween, pH 7.4 for 15 minutes and once with 5% (w/v) non-fat dry milk in TBS-Tween, pH 7.4 for 20 minutes with agitation. The incubation with the appropriate Horseradish Peroxidase conjugated secondary antibody diluted 1:7500 in 5% (w/v) non-fat dry milk in TBS-Tween, pH 7.4 was performed at room temperature for 1.5 hours with agitation. Membrane was then washed three times with TBS-Tween, pH 7.4 for 15 minutes followed by a wash with PBS, pH 7.4 for 10 minutes. Immunodetection of membrane was performed using Amersham ECL Advance Western Blotting Detection Kit. Equal quantities of detection solutions A and B were mixed and pipette on to the membrane. After 1 minute incubation, detection mix was discarded and the membranes were wrapped with stretch film and chemiluminescent signal was detected via chemiluminescence imaging system (DNR Systems MF-ChemiBIS 3.2, Israel).

To ensure loading of equal protein into wells, the membranes were stripped with stripping buffer 62.5 mM Tris-HCl, pH 6.7 containing 100 mM 2-mercaptoethanol, 2% (w/v) SDS to remove the antibody from the membrane. The membrane in stripping buffer was incubated at 50°C and then washed twice with large volumes of TBS-Tween, pH 7.4 for 15 minutes. Following the block of the membrane in blocking buffer for 1 hour at room temperature, the membrane was incubated with primary antibody (β-actin antibody diluted in blocking buffer 1:2500 dilution) as described above. After the Horseradish Peroxidase conjugated secondary antibody incubation (1:5000 dilution in blocking buffer) immunodetection of the membrane was visualized via chemiluminescence imaging system as described above.

3.6. STATISTICAL ANALYSIS

For the statistical analysis of the expression results of RCC patients, MedCalc Statistical Software program (version 11.6.1.0) was used. The Wilcoxon test was used to analyze the gene expression results from the healthy tissues versus the autologous tumor tissues. However, Mann-Whitney test was applied to evaluate the gene expression results

when comparing the patient groups. The differences between the gene expression results of cell lines were analyzed using student's t-test. The TG2 activity results of patients and cell lines were also examined using student's t-test. Student's t-test analyses were performed in GraphPad Prism (version 5.03) analysis program. All results were considered statistically significant when $P<0.05$. The calculations of the statistical analysis were shown in Appendix section.

4. RESULTS

4.1. TG2, SYNDECAN-4, AND INTEGRIN β1 GENE EXPRESSION IN RCC PATIENTS

The expression levels of TG2, syndecan-4 and integrin β1 were analyzed in 61 RCC patients by comparing the expression levels in tumor tissues and healthy counterparts. For this purpose, RNA was isolated from freshly frozen kidney tumor and healthy tissues and the expression levels of TG2, syndecan-4 and integrin β1 were analyzed by the quantitative real-time PCR. Individual data points in the following graphs correspond to each patient's average expression value of the interested gene normalized against the 18SrRNA. Each data point was derived from at least three experiments performed in duplicate.

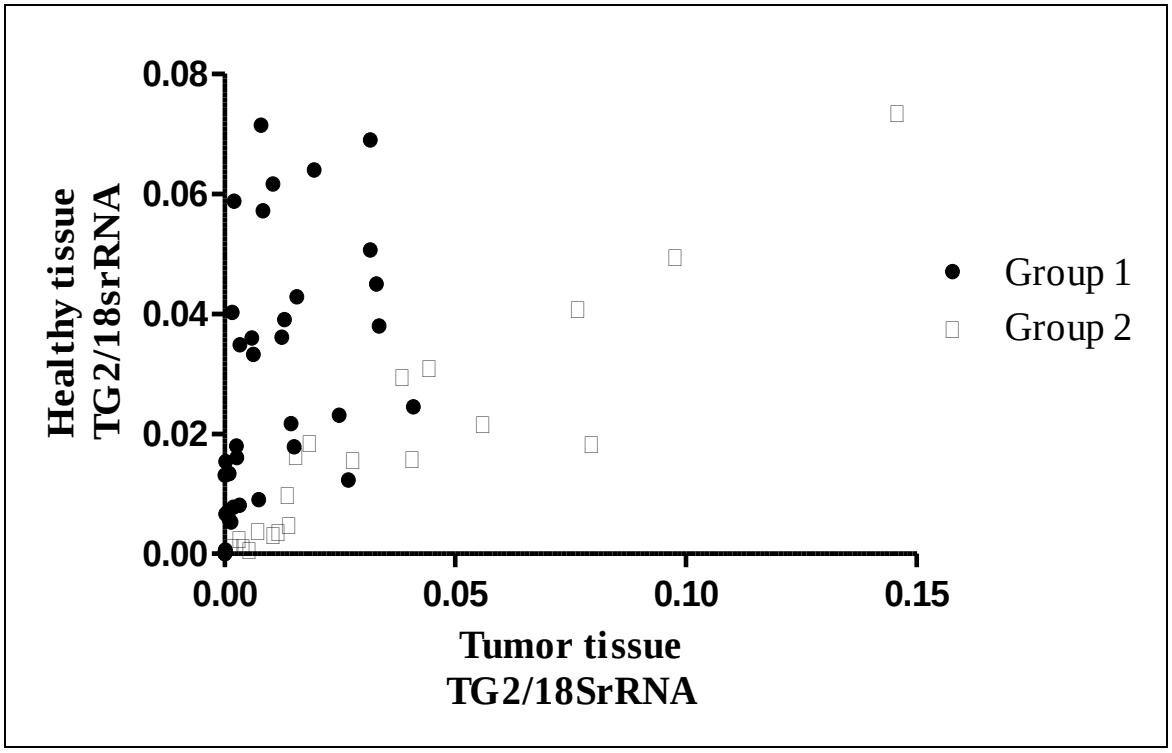

Figure 4.1. The expression levels of TG2 in healthy and tumor tissue samples. Each point represents the mean TG2 expression value for a RCC patient. In Group 1 (n=40), mean value of TG2 expression and standard error of the mean (S.E.M.) in healthy and tumor tissues were 0.025±0.003 and 0.009±0.002, respectively. *P* values between healthy and tumor tissues of Group 1 was $P<0.0001$. In Group 2 (n=21), mean value and S.E.M. in healthy and tumor tissues were 0.018±0.004 and 0.035±0.008, respectively. *P* values between healthy and tumor tissues of Group 2 was $P=0.0001$.

TG2 expression was studied in 61 RCC patients comparing the expression levels in tumor tissues and healthy counterparts. In Figure 4.1, Group 1 represents the patients that show lower TG2 expression in the tumor tissue compared to the healthy tissue ($P<0.0001$, Wilcoxon test). Group 2 represents patients that show increased TG2 expression in tumor tissue in comparison to the healthy tissue ($P=0.0001$, Wilcoxon test). Out of 61 patients, 21 patients (34%) showed an increased TG2 expression in the tumor tissue when compared with the corresponding healthy tissue while 66% of the patients (40 patients) showed decreased TG2 expression in the tumor tissue in comparison to the control tissue. The mean TG2 expression value in the tumor tissues from Group 2 was significantly higher than that of Group 1 ($P=0.0001$, Mean-Whitney test).

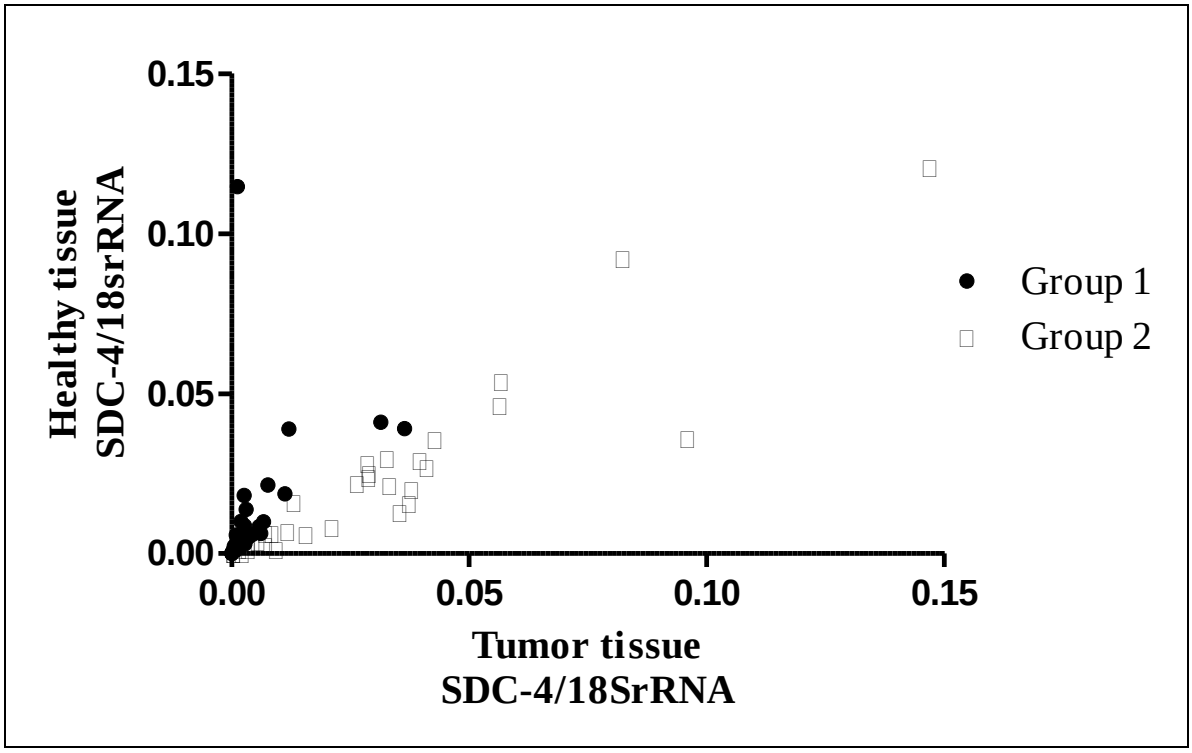

Figure 4.2. The expression levels of syndecan-4 (SDC-4) in healthy and tumor tissue samples. Each point represents the mean syndecan-4 expression value for one RCC patient. In Group 1 (n=29), mean value of syndecan-4 expression and S.E.M. in healthy and tumor tissues were 0.014±0.004 and 0.005±0.002, respectively. *P* values between healthy and tumor tissues of Group 1 was $P<0.0001$. In Group 2 (n=32), mean value and S.E.M. in the healthy and tumor tissues were 0.022±0.005 and 0.03±0.006, respectively. *P* values between healthy and tumor tissues of Group 2 was $P<0.0001$.

Analysis of the tumor samples for syndecan-4 expression showed that two distinct populations were present in our patient pool as shown in Figure 4.2. Group 1 represents the patients that show lower syndecan-4 expression in the tumor tissue in comparison to the healthy control tissue ($P<0.0001$, Wilcoxon test). Group 2 represents the patients that show increased syndecan-4 expression in the tumor tissue compared to the healthy tissue ($P<0.0001$, Wilcoxon test). Group 1 comprises the 48% of patients (29 patients) and Group 2 accounts for the 52% of patients (32 patients). The average syndecan-4 expression value in tumor tissues was found to be significantly higher in Group 2 when compared to Group 1 ($P<0.0001$, Mann-Whitney test).

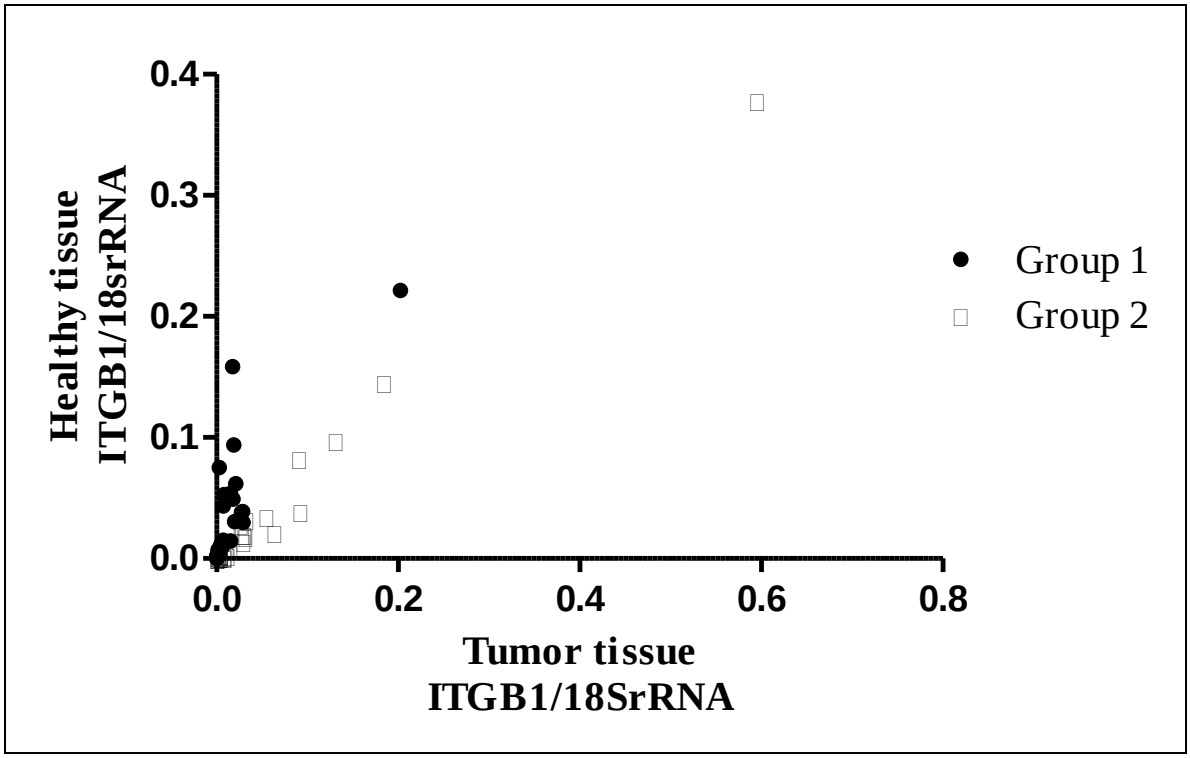

Figure 4.3. The expression levels of integrin β1 (ITGB1) in healthy and tumor tissue samples. Each point represents the mean integrin β1 expression value for one RCC patient. In Group 1 (n=34), the mean value of integrin β1 expression and S.E.M. in healthy and tumor tissues were 0.031±0.008 and 0.014±0.006, respectively. *P* values between healthy and tumor tissues of Group 1 was $P<0.0001$. In Group 2 (n=32), mean value and S.E.M. in healthy and tumor tissues were 0.036±0.015 and 0.055±0.022, respectively. *P* values between healthy and tumor tissues of Group 2 was $P<0.0001$. Due to scaling of the graph in Figure 4.3 one of the data points stays out of the graph range.

The expression of integrin β1 in 61 RCC patients was also analyzed as demonstrated in Figure 4.3. Group 1, which represents the increased expression of integrin β1 in healthy tissues with respect to tumor tissues ($P<0.0001$, Wilcoxon test), accounts approximately for the 56% of all population (34 patients). Group 2 demonstrating the increased expression of integrin β1 in tumor tissues compared to healthy tissues ($P<0.0001$, Wilcoxon test) constitutes 44% of the patients (27 patients). The average integrin β1 expression value in tumor tissues of Group 2 was significantly higher than that for Group 1 ($P=0.0034$, Mann-Whitney test). Due to scaling of the graph in Figure 4.3 one of the data points stays out of the graph range.

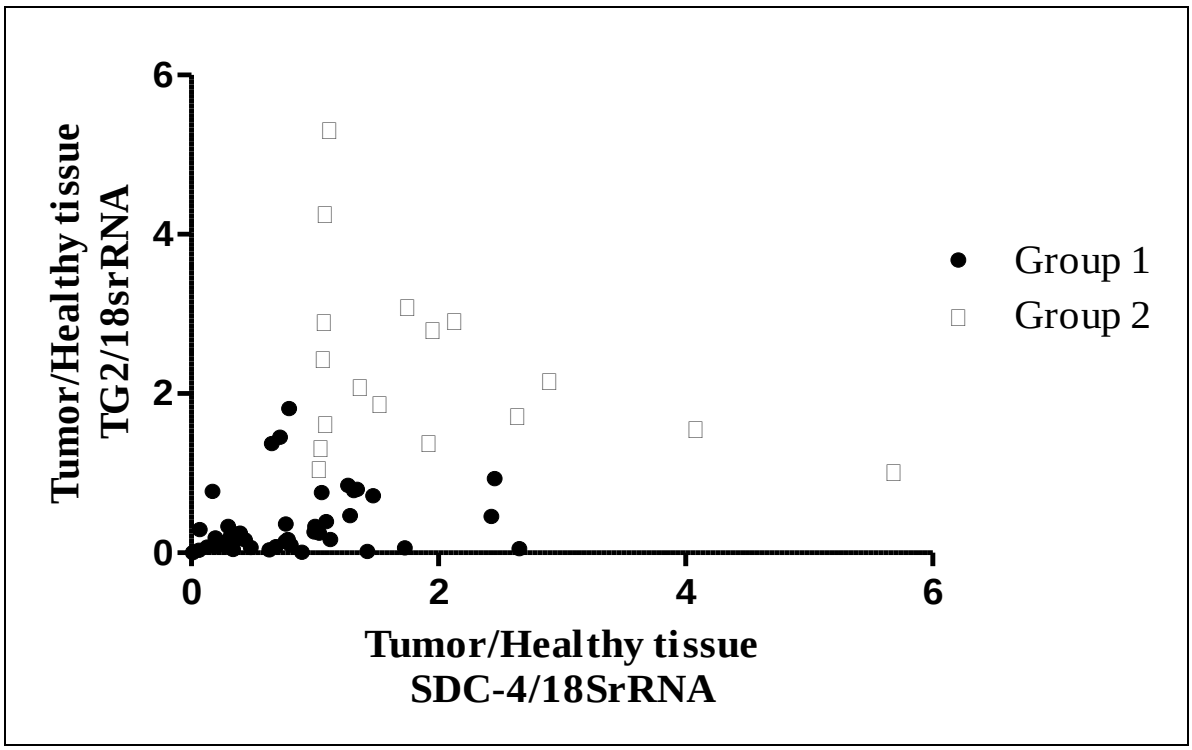

Figure 4.4. Expression levels of TG2 and syndecan-4 (SDC-4) evaluating tumor/healthy tissue ratio. Each point represents the mean expression ratio (tumor/healthy) value of TG2 (y axis) and syndecan-4 (x axis) for one RCC patient. In Group 1 (n=44), the mean value and S.E.M. of TG2 and syndecan-4 expression ratio (tumor/healthy) were 0.411±0.072 and 0.815±0.096, respectively. In Group 2 (n=17), the mean value and S.E.M. of TG2 and syndecan-4 expression ratio (tumor/healthy) were 2.344±0.279 and 1.968±0.308, respectively. *P* values between Group 1 and Group 2 for both TG2 and syndecan-4 expression ratio was $P<0.0001$.

For the purpose of correlation analysis between TG2 and syndecan-4, gene expression ratios for TG2 and syndecan-4 were plotted against each other for each patient. Figure 4.4 shows that there are two distinct groups. Group 1 represents the patients that demonstrate low tumor/healthy ratio both for TG2 and syndecan-4, and the patients with increased expression level detected either only for TG2 or syndecan-4 in the tumor tissue compared to the healthy tissue.

Group 2 represents the patients demonstrating increased expression levels both for TG2 and syndecan-4 simultaneously in their tumor tissue compared with the healthy

counterparts. In other words, 80% patients in the population that show increased TG2 expression also show increased syndecan-4 expression in the tumor tissue in comparison to the healthy tissue. Statistical analysis showed that the mean expression ratio values of TG2 and syndecan-4 was significantly high in Group 2 when compared to Group 1 ($P<0.0001$ and $P<0.0001$, respectively, Mann-Whitney test).

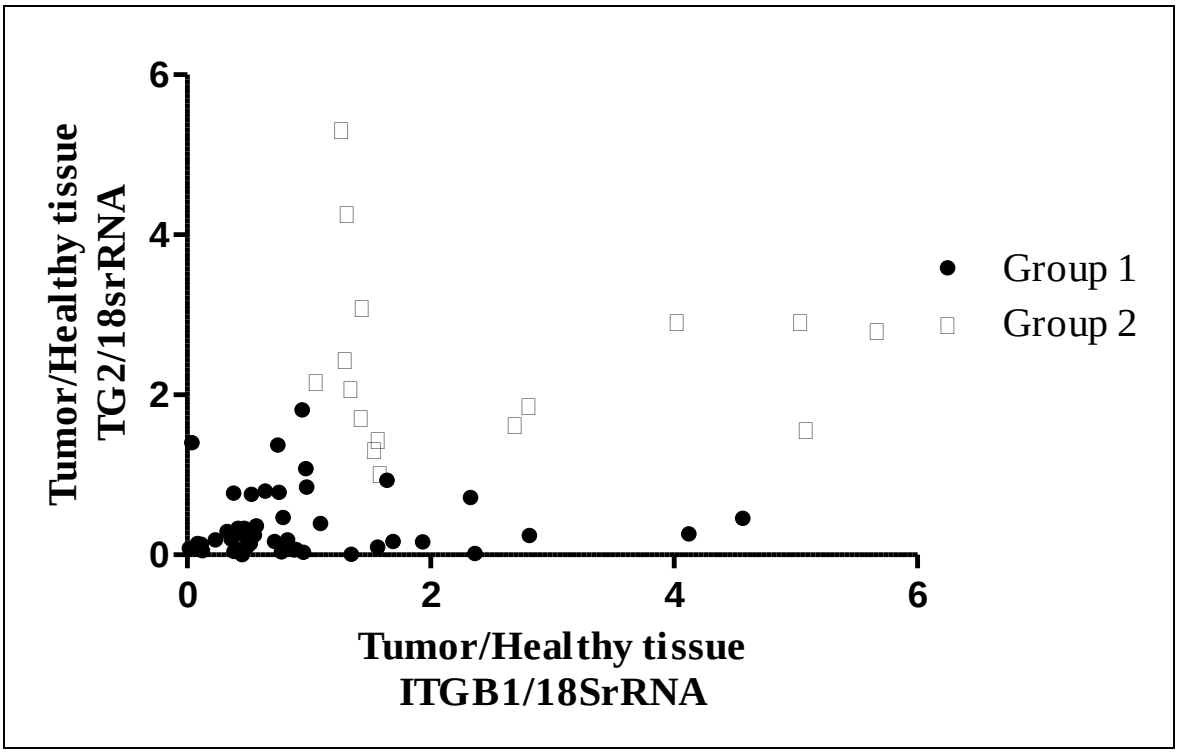

Figure 4.5. Expression levels of TG2 and integrin β1 (ITGB1) evaluating tumor/healthy tissue ratio. Each point represents the mean value of TG2 (y axis) and integrin β1 (x axis) expression ratio (tumor/healthy tissue) for one RCC patient. In Group 1 (n=43), the mean value and S.E.M. of TG2 and integrin β1 expression ratio (tumor/healthy tissue) were 0.356±0.056 and 0.972±0.151, respectively. In Group 2 (n=18), the mean value and S.E.M. of TG2 and integrin β1 expression ratio (tumor/healthy tissue) were 2.368±0.255 and 2.302±0.368, respectively. *P* values between Group 1 and Group 2 for both TG2 and integrin β1 expression ratio was $P<0.0001$.

In order to analyze the association between TG2 and integrin β1, the expression values for these genes were plotted against each other in the graph presented in Figure 4.5. Group 1 illustrates the patients that show low TG2 or integrin β1 expression in tumor

tissue compared to healthy tissue, and patients with increased expression level detected only for TG2 or integrin β1 in the tumor tissue when compared to the healthy tissue.

Group 2 represents the patients demonstrating increased expression levels both for TG2 and integrin β1 simultaneously in their tumor tissue compared to the healthy counterparts.

In other words, when the expression levels for TG2 and integrin β1 was compared between the tumor tissue and healthy counterparts for the Group 2, in 86% of patients increased TG2 expression was accompanied by increased expression levels of integrin β1.

Statistical analysis showed that the average expression ratio values of TG2 and integrin β1 was significantly high in Group 2 when compared to Group 1 ($P<0.0001$ and $P<0.0001$, respectively, Mann-Whitney test).

4.2. TG2 ACTIVITY IN RCC PATIENTS

Enzymatic activity of TG2 in tissue lysates were measured by BTC incorporation into casein. TG2 activity was measured by incubation of tissue lysates on casein coated surfaces in the presence of BTC as described in the Method Section 3.4.1. Following the addition of extravidin peroxidase which binds with high affinity and specificity to BTC and the reaction was visualized by the addition of the colorgenic substrate of peroxidase TMB.

Firstly optimum amount of protein that will be used in the assay was determined using the Bradford assay as presented in Figure 4.6.

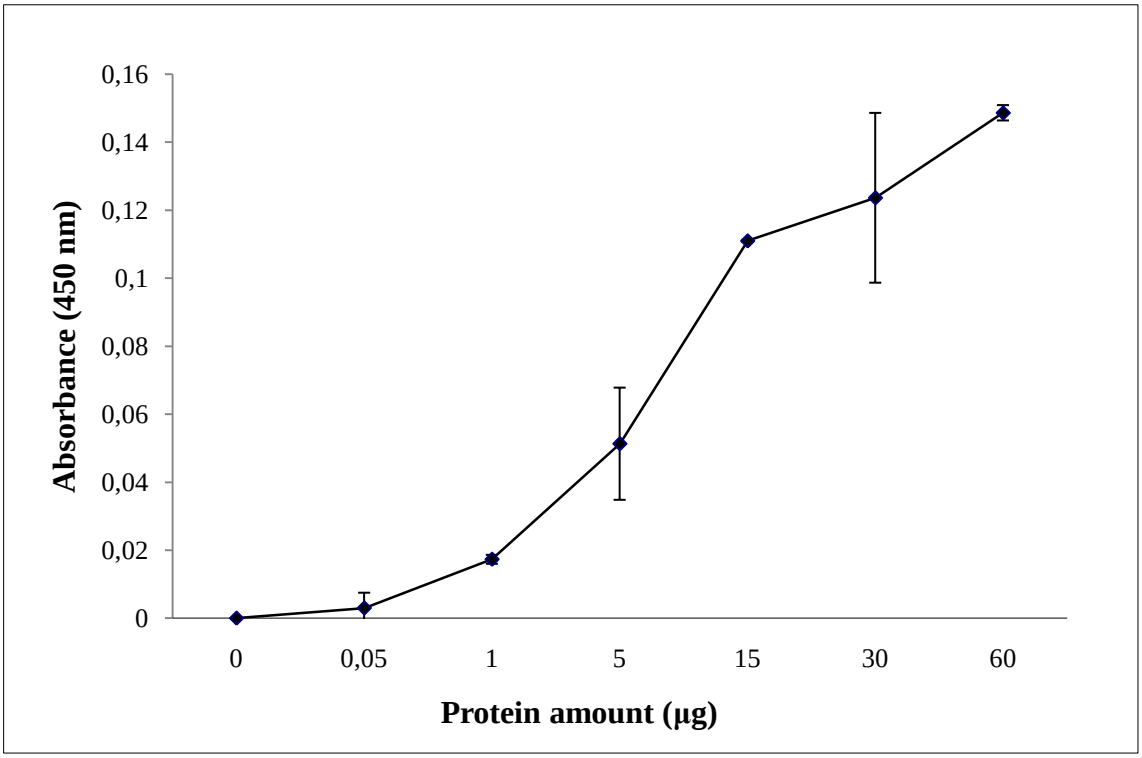

Figure 4.6. Measurement of TG2 activity in samples containing different amount of protein

Each point data corresponds to the mean absorbance values at 450 nm ± standard deviation (S.D.) which was performed in triplicate. 0.05 µg, 1 µg, 5 µg, 15 µg, 30 µg, 60 µg protein samples were analyzed for TG2 activity. As values after 15 µg protein sample showed absorbance that have reached to a saturation plateau, 15 µg protein sample was used for further assays.

In order to measure the TG2 activity, 10 randomly selected patients from the Group 1 and the Group 2, which was shown in the Figure 4.1, was used in the activity assays. More specifically, TG2 activity was measured in the patient Group 1 that shows high TG2 expression in healthy tissue in comparison to the tumor tissue (Figure 4.7) and in the patient Group 2 (Figure 4.8) which is characterized by high tumor TG2 expression versus the control healthy tissues. 10 patients were randomly selected for each group.

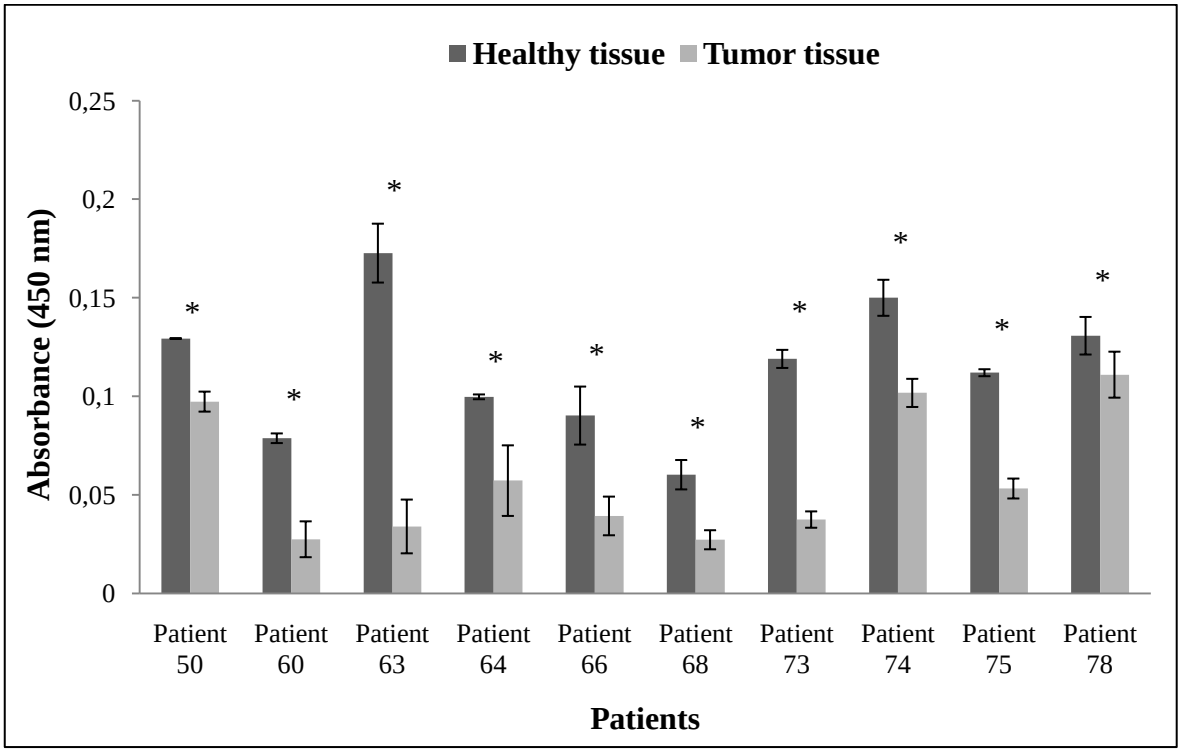

Figure 4.7. The measurement of TG2 activity in randomly selected 10 patients from Group 1 that show high TG2 expression in healthy tissue with respect to tumor tissue. Each column corresponds to the mean value of TG2 activity assay results performed in healthy and tumor tissues of selected patients and standard deviation. Experiment was performed in triplicate and * symbol indicates the statistically difference between healthy and tumor tissues (P<0.05).

The patients who were selected from the Group 1 demonstrated an increased TG2 activity in their healthy tissues when compared to their tumor tissues as seen in the Figure 4.7 (P<0.05, student's t-test).

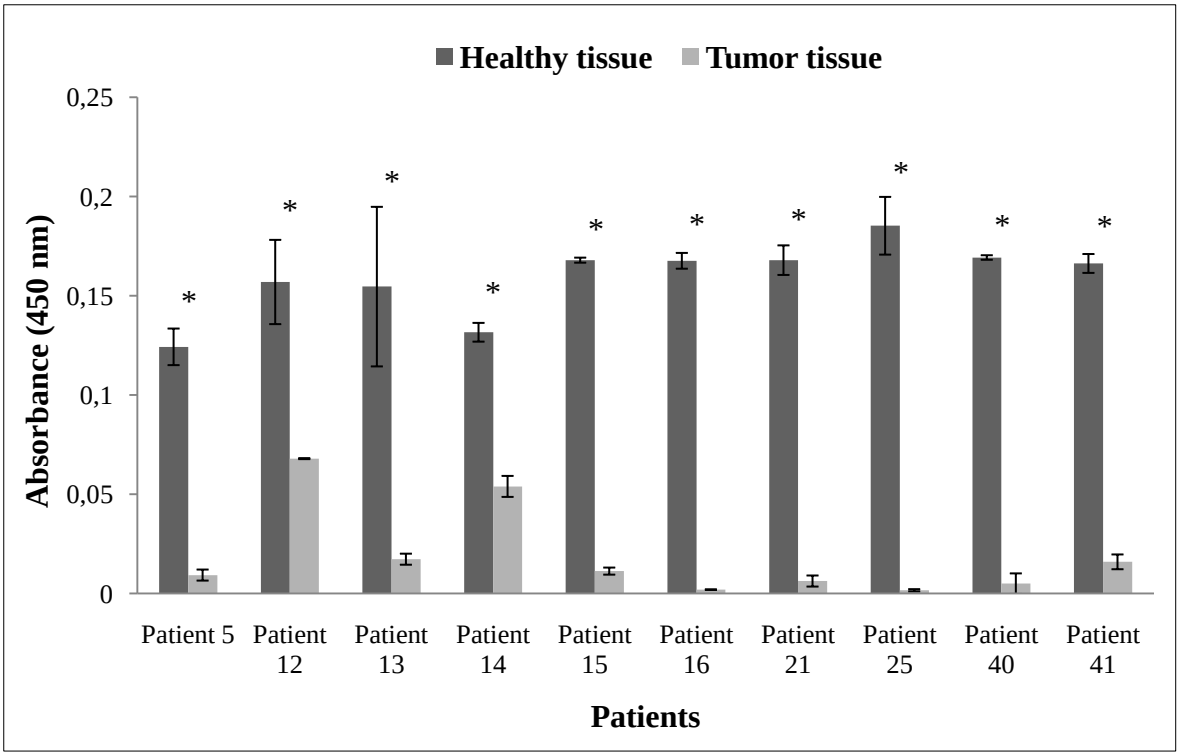

Figure 4.8. The measurement of TG2 activity in randomly selected 10 patients from Group 2 that show high TG2 expression in tumor tissue compared to healthy tissue. Each column corresponds to the mean value of TG2 activity assay results performed in healthy and tumor tissues of selected patients and standard deviation. Experiment was performed in triplicate and * symbol indicates the statistically difference between healthy and tumor tissues ($P<0.05$).

All randomly selected 10 patients from Group 2 showed increased TG2 activity in the healthy tissues when compared to the tumor tissues as represented in the Figure 4.8 ($P<0.05$, student's t-test).

4.3. TG2, SYNDECAN-4, AND INTEGRIN β1 GENE EXPRESSION IN CONTROL AND RCC CELL LINES

The real-time PCR was conducted also in control RPTEC, Caki-2, and A-498 RCC cell lines to analyze expression levels of TG2, syndecan-4 and integrin β1. Figure 4.9, 4.10 and 4.11 show the expression level values for each gene ± S.D. which was performed in duplicate.

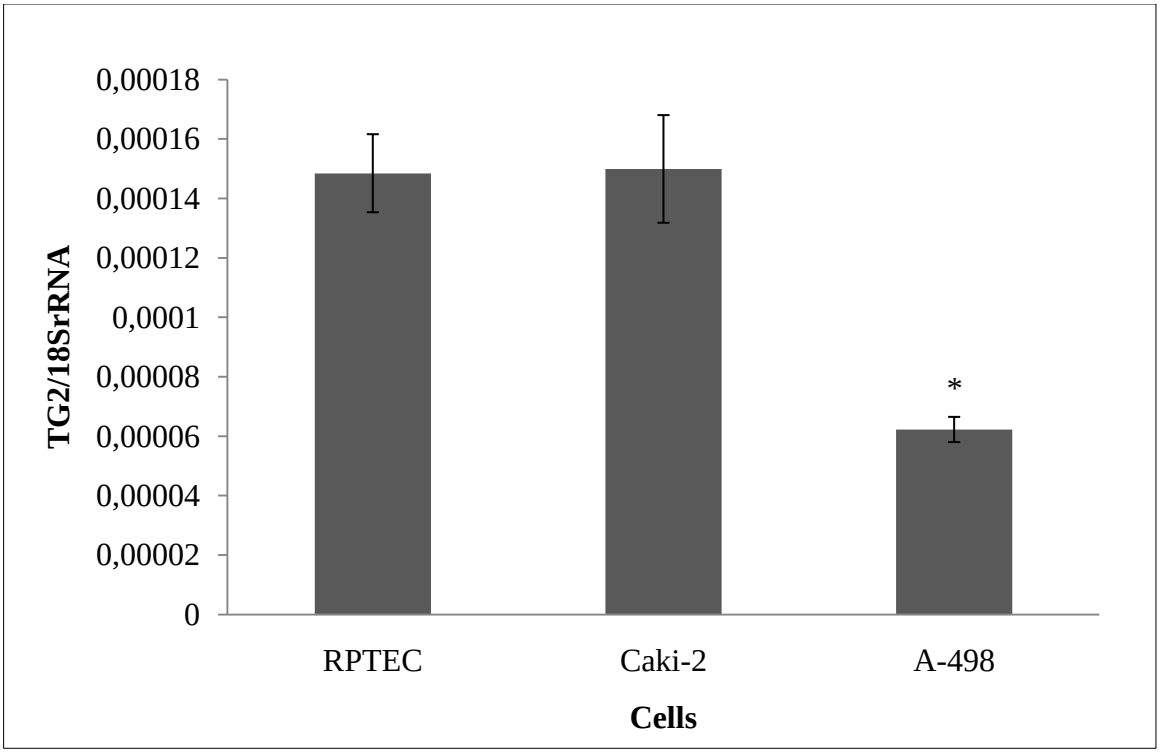

Figure 4.9. TG2 expression levels in RPTEC, Caki-2, and A-498 cell lines. Each column corresponds to the expression level values of TG2 in cell lines and standard deviation. Experiment was performed in duplicate and * symbol indicates the statistically difference of A-498 from RPTEC and Caki-2 ($P<0.05$).

Control RPTEC and Caki-2 cells showed a similar TG2 expression, however, A-498 cells showed decreased TG2 expression level compared the control RPTEC and Caki-2 cells as shown in the Figure 4.9 ($P<0.05$, student's t-test).

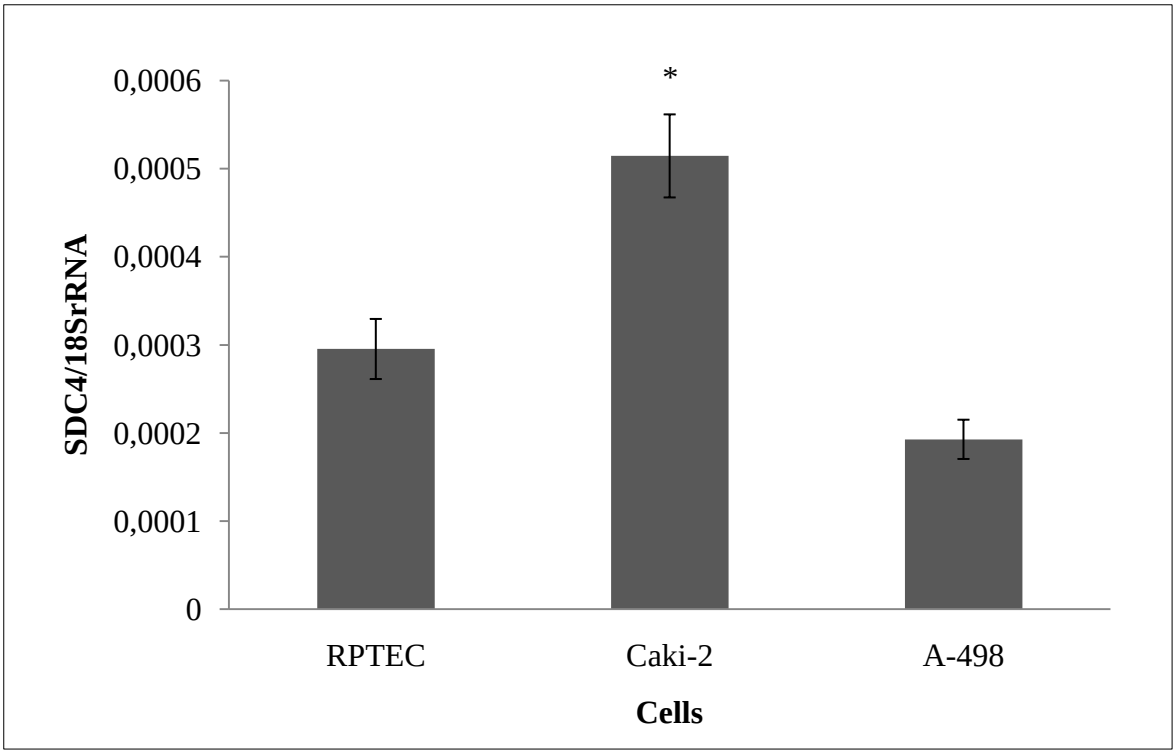

Figure 4.10. Syndecan-4 (SDC-4) expression levels in RPTEC, Caki-2, and A-498 cells. Each bar corresponds to the expression level values of TG2 obtained for the cell lines and standard deviation. Experiment was performed in duplicate and * symbol indicates the statistically difference of Caki-2 from RPTEC and A-498 (P<0.05).

Figure 4.10 shows that Caki-2 has increased syndecan-4 expression when compared to RPTEC and A-498 cells (P<0.05, student's t-test). Control RPTEC cell line also showed an increased syndecan-4 expression in comparison to A-498 cells (statistically not significant).

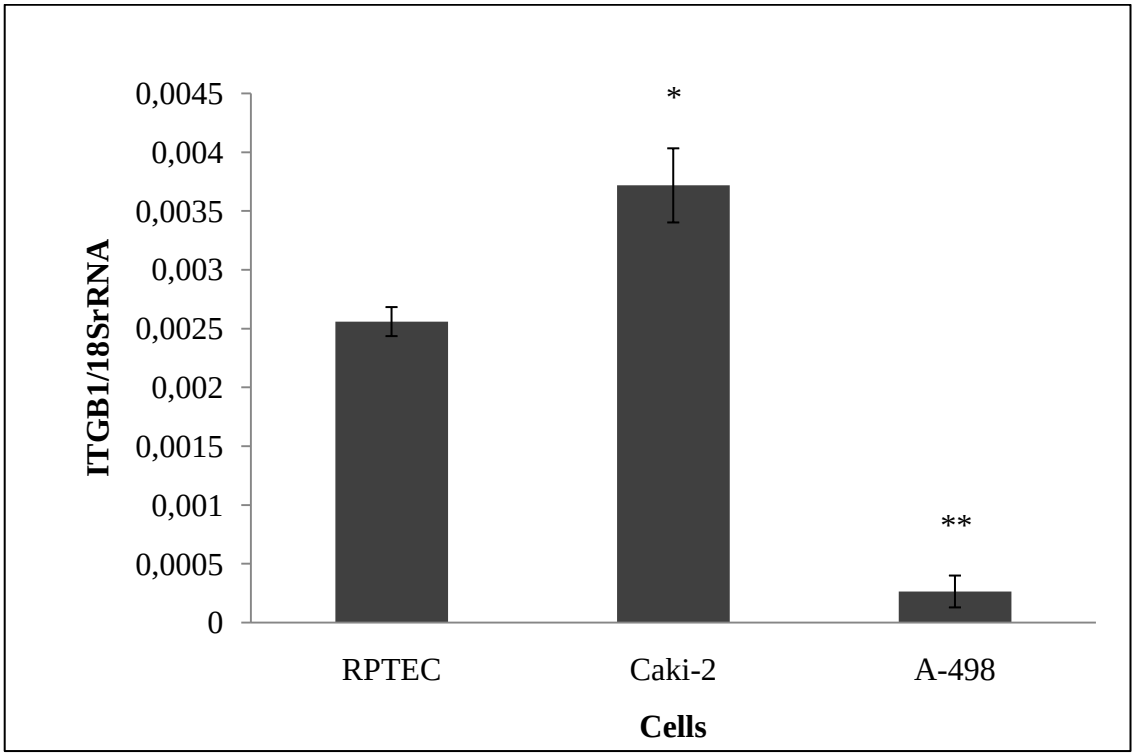

Figure 4.11. Integrin β1 (ITGB1) expression levels in RPTEC, Caki-2, and A-498 cell lines. Each column corresponds to the expression level values of ITGB1 for the cell lines and standard deviation. Experiment was performed in duplicate and * symbol indicates the statistically difference of Caki-2 from RPTEC and A-498 (P<0.05). ** symbol indicates the statistically difference of A-498 from RPTEC and Caki-2.

Similar to results for syndecan-4 expression, Caki-2 cells showed increased integrin β1 expression when compared to other cell lines (P<0.05). A-498 cells showed a remarkable decreased expression of integrin β1 in comparison to RPTEC and Caki-2 cells as shown in the Figure 4.11 (P<0.05).

4.4. TG2 ACTIVITY IN RPTEC, CAKI-2, AND A-498 CELL LINES

After the incubation of control RPTEC, Caki-2, and A-498 RCC cells on FN coated surfaces in the presence of BTC, the amount of biotin incorporated into FN matrix was measured as described in the Method Section 3.4.2.

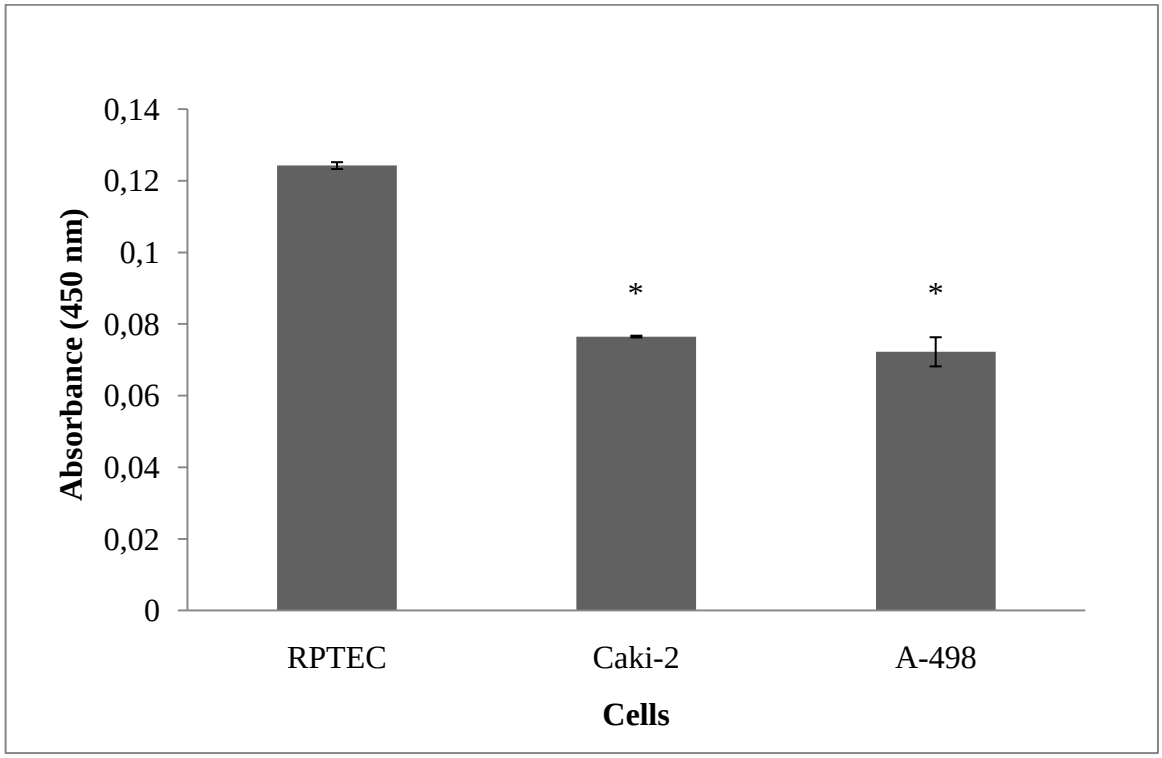

Figure 4.12. Cell surface TG2 activity in RPTEC, Caki-2, and A-498 cells. Each column corresponds to the mean value of TG2 activity obtained for the cell lines and standard deviation. . Experiment was performed in quadruplicate and * symbol indicates the statistically difference of Caki-2 and A-498 from RPTEC (P<0.05).

RPTEC cells exhibited increased cell surface TG2 activity compared to the RCC cancer cell lines. Caki-2 and A-498 cancer cells showed similar cell surface TG2 activity which was 1.6 fold lower than that of RPTEC cells (P<0.05).

4.5. TG2, SYNDECAN-4, AND INTEGRIN β1 PROTEIN EXPRESSION ANALYSIS IN RPTEC, CAKI-2, AND A-498 CELL LINES

In order to analyze TG2, syndecan-4 and integrin β1 protein expressions in RPTEC, Caki-2, and A-498 cell lines, total cell lysates obtained from cell lines were separated on SDS-PAGE and transferred to nitrocellulose membrane and probed with anti-TG2 (1:5000 dilution), anti-syndecan-4 (1:7500), anti-integrin β1 (1:7500) and anti-β-actin (1:2500) antibodies as seen in the Figure 4.13.

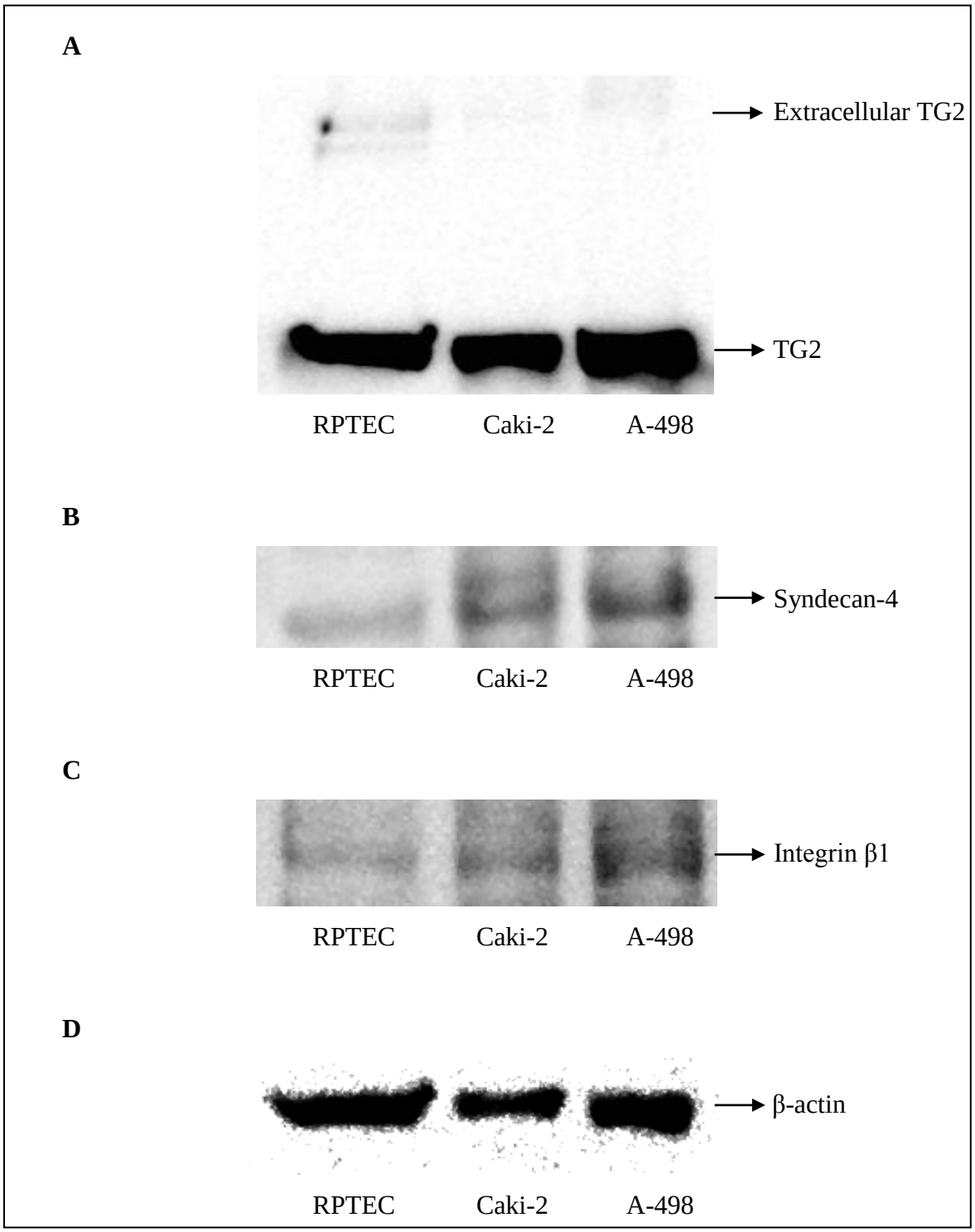

Figure 4.13. Western Blot analysis in cell lines **A.** TG2, **B.** Syndecan-4, **C.** Integrin β1, and **D.** β-actin blots

In agreement with the real-time PCR results RPTEC cells exhibited increased TG2 protein expression compared to the A-498. Interestingly, TG2 protein deposition to the ECM was only evident in the control RPTEC cells. Syndecan-4 and integrin β1 protein

expression levels were consistent with the gene expression results of RPTEC, Caki-2, and A-498 cells obtained from the real-time PCR analysis (Figure 4.9 and 4.10).

5. DISCUSSION

RCC is the most abundant type of kidney cancer and demonstrates resistance to the radiotherapy and chemotherapy [11]. To date there has been no study examined the role of TG2 in RCC hence this study is the first to investigate the importance of TG2 in RCC.

TG2 can function as an ECM stabilizer when deposited into the extracellular environment by stimulating the activation of latent TGF-β to active form [39]. TGF-β increases ECM protein deposition by inducing the production of ECM proteins while inhibiting ECM degradation not only through reducing the MMP synthesis but also through increasing the inhibitors of MMPs, TIMPs [37, 38, 81]. TGF-β activity also increases TG2 expression as it enhances transcriptional activity of the TG2 promoter [82]. In addition to the effects of TG2 on matrix deposition via TGF-β signaling, TG2 crosslinks the ECM proteins using its transamidating activity and ECM becomes consequently more resistant to degradation of MMP enzymes [19].

Early studies reported that primary tumors of breast cancer, and primary melanoma cell line show decreased expression of TG2 [72, 75, 83] and also some studies showed that decreased TG2 expression and activity contributes to the primary tumor progression by destabilizing the ECM [79, 84]. Similar to these previous results, in this study 67% of the primary RCC tumors showed a decrease in the TG2 expression. Given that the activation of TGF-β by TG2 leads to an increase in ECM deposition and the TG2 over-expression generates a MMP resistant ECM through crosslinking, these results suggest that primary tumors need to downregulate the TG2 expression in order to render their ECM more susceptible to MMP degradation which is necessary for the tumor growth. In support of this hypothesis, TG2 activity assay results showed that patients showing a high TG2 expression ratio for healthy/tumor also exhibited a high TG2 activity ratio for healthy tissues in comparison to the tumor tissues.

Accumulating evidence indicated that increased TG2 in association with increased integrin β1 expression correlates with an increased drug resistance and metastatic potential [73, 74]. *In vitro* studies showed that TG2 does not act as an ECM stabilizer when it is co-

localized with integrins. Independent from its transamidating activity, TG2 binds to FN and TG2-FN complex interacts with integrins [41, 85]. Moreover, a recent work showed that FN bound TG2 interacts with the heparan sulfate chains of syndecan-4 cell surface receptor and acts as a novel cell adhesion protein [86]. This binding mediates the activation of integrin β1 by the inside-out signaling route and promotes the cell survival [42].

In agreement with the recent literature, in this study 34% of RCC tumor tissues showed high expression levels of TG2 when compared to the healthy tissues. Moreover, in 71% of the patients, increased TG2 expression was accompanied by increased expression levels of syndecan-4 and integrin β1. These results suggest that increase in syndecan-4 and integrin β1 expression is accompanied by an increase chance of TG2 interaction with these molecules. In this case, TG2 loses its activity, interacts with syndecan-4 and initiates integrin β1 dependent cell adhesion/migration and survival. Therefore, when overexpressed simultaneously with syndecan-4 and integrin β1, TG2 rather than acting as a matrix stabilizer, would act as a novel cell adhesion protein and confer increased cell survival, and invasiveness to the primary tumors. In support of this hypothesis, TG2 activity assay results showed that TG2 activity was diminished in tumors which showed a high TG2 expression in parallel with high integrin β1 and syndecan-4 expression when compared to the counterpart control tissues.

In order to confirm the results obtained from tissues, cell lines were used for an *in vitro* approach. Caki-2 and A-498 cell lines were used as primary RCC cancer model and RPTEC cell line was used as the control cell line.

Expression results showed TG2 expression levels in RPTEC and Caki-2 are similar while A-498 cells showed a decreased expression of TG2 compared to the other cell lines. In addition, A-498 cell line showed both decreased expression levels of syndecan-4 and integrin β1 compared to RPTEC and Caki-2 cells. Moreover, TG2 activity assay results demonstrated that A-498 cells showed decreased crosslinking activity compared with the RPTECs. Given that majority of patients showed a decrease in the TG2 expression in their tumors in comparison to the healthy tissue (Figure 4.1, Group 1), A-498 mimic the primary tumor tissues of these patients and exhibited a decreased TG2 activity and expression when compared to the RPTEC. A-498 cells also exhibited lower expression of syndecan-4 and

integrin β1 than RPTEC in agreement for the expression pattern of these genes observed in the majority of patients (Figure 4.1, Group1).

Caki-2 cells also showed increased expression of TG2, syndecan-4 and integrin β1 when compared to RPTEC and A-498 cell lines. Increased TG2 expression together with the increased syndecan-4 and integrin β1 expressions in Caki-2 cells may be an indicator of metastatic behavior. Caki-2 has a metastatic counterpart cell line called Caki-1 isolated from the same patient [87]. The study by Strefford *et. al.* revealed that Caki-2 shares some of the same chromosome aberrations with the metastatic Caki-1 RCC cell line isolated from skin metastasis [87] supporting the idea that Caki-2 cell line has metastatic potential and may metastasize a distant organ similar to metastatic site where Caki-1 isolated. The results obtained from Caki-2 also support our hypothesis about the patients showing high TG2, syndecan-4, and integrin β1 expression and the decreased TG2 activity in tumor tissues due to the interaction of TG2 with syndecan-4. This TG2-syndecan-4 interaction would lead to the activation of integrin β1 signaling resulting in an increase of cell survival and the ability of metastasis. Caki-2 also showed decreased crosslinking activity compared to control RPTECs supporting the activity results of patients revealing increased TG2 activity in healthy tissues in comparison to tumor tissues.

6. CONCLUSION

In summary, it can be concluded that primary tumors possibly downregulate TG2 expression to contribute to MMP degradation in ECM during the tumor growth. In contrast, the primary tumors might increase TG2 expression together with the expression of syndecan-4 and integrin β1 to support cell adhesion/migration and survival to gain invasiveness and metastatic potential. In support of this hypothesis, TG2 activity assay results showed that TG2 activity was diminished not only in tumors with decreased TG2 expression but also in tumors which showed a high TG2 expression in parallel with high integrin β1 and syndecan-4 expression. *In vitro* approach of RCC and control cell line support the results of tissue samples since the expression results of TG2, syndecan-4, and integrin β1 and the TG activity results obtained from RPTEC, Caki-2, and A-498 cell lines were in parallel with the observations from the patient tissue samples. In other words, majority of RCC tumors down regulated the TG2 while a small population which might have a metastatic potential up regulated TG2 together with syndecan-4 and integrin β1 where TG2 can act as signaling molecule and possibly increases cell survival and invasiveness.

7. FUTURE DIRECTIONS

This work is the first study that represents the role of TG2 in RCC primary tumors. The future prospects of the project includes the investigation of TG2, syndecan-4 and integrin β1 expression along with TG2 activity in the RCC tumors isolated from the metastatic site and determine the association of TG2 with integrin β1 and syndecan-4 in these tissues.

In *in vitro* studies Caki-2 as primary RCC model and Caki-1 as metastatic RCC model can be used and TG2 expression together with syndecan-4 and integrin β1, TG2 activity and also co-localization of TG2 and integrin β1 in ECM might be investigated. Furthermore, Caki-2 cells may be compared with Caki-1 in terms of the metastatic potential through the cell migration assays to assess the contribution of TG2 to the metastatic behavior suggesting the possible usage of TG2 as a marker that indicates the metastatic potential of the RCC tumors.

APPENDIX

Table A.1. Histopathological evaluation and other features of RCC patients:

Patient Code	Gender	Age	Stage	Fuhrmann Grade	RCC subtype
1	F	81	T1bNxM0	Grade 3	clear cell
3	F	49	T1bN0M0	Grade 3	clear cell
5	F	51	T1bN0M0	Grade 3	clear cell
6	F	56	T3bNXM1	Grade 4	clear cell
7	M	53	T1bNxM0	Grade 2	clear cell
10	M	68	T1aNxM1	Grade 3	clear cell
11	M	73	T1bNxM0	Grade 3	chromophobe
12	M	59	T1aNxM0	Grade 2	clear cell
13	M	45	T1bNxM0	Grade 2	chromophobe
14	M	62	T3bN0M1	Grade 4	-
15	F	67	T1aNxM0	Grade 2	clear cell
16	F	71	T3bNxM0	Grade 3	clear cell
19	M	46	T2NxM0	Grade 2	clear cell
21	M	54	T3bNxM1	Grade 4	clear cell
25	M	62	T1aNxM0	Grade 2	clear cell
27	F	53	T1aNxM0	Grade 2	clear cell
30	M	81	T1N0M0	Grade 3	papillary
34	F	83	T2NxM0	Grade 3	papillary
35	F	66	T1aNxM0	Grade 3	clear cell
36	M	72	T3bNxM1	Grade 3	clear cell
37	M	50	T1bN0M0	Grade 3	clear cell
39	M	59	T3bNXM0	Grade 4	clear cell
40	F	57	T1aN0M0	Grade 2	clear cell
41	F	63	T1bNxM0	Grade 4	clear cell
42	F	72	T3aNxM1	Grade 4	clear cell
43	M	67	T2NxM0	Grade 3	chromophobe
44	M	44	T1bNxM0	Grade 2	clear cell
45	M	50	T3aN0M1	Grade 4	clear cell
46	M	55	T2NxM0	Grade 4	clear cell
47	F	55	T3bN0M1	Grade 4	clear cell
48	M	59	T2NxM0	Grade 2	clear cell
49	M	50	T1bNxM0	Grade 2	papillary
50	M	66	T3bNxMx	Grade 3	clear cell
51	F	77	T2NxMx	Grade 2	papillary
52	M	70	T1bNxMx	-	clear cell

Table A.1. Histopathological evaluation and other features of RCC patients: (continue)

53	F	61	T3bNxM0	Grade 3	clear cell
54	M	79	T2N0Mx	Grade 2	clear cell
55	M	50	T2NxMx	Grade 3	clear cell
56	M	47	T1bNxMx	Grade 2	clear cell
57	M	57	T3bNxMx	Grade 4	papillary
58	F	42	T2NxMx	Grade 3	chromophobe
60	M	57	T3bNxMx	Grade 3	clear cell
61	M	52	T1aNxMx	Grade 2	clear cell
62	M	57	T1aN0M0	Grade 2	clear cell
63	M	66	T1bNxMx	Grade 3	clear cell
64	M	45	T3bNxMx	Grade 3	clear cell
65	M	69	T3bNxMx	Grade 2	clear cell
66	M	50	T3aNxMx	Grade 2	clear cell
67	M	60	T2N0Mx	Grade 3	chromophobe
68	F	70	T2N0Mx	Grade 3	clear cell
69	F	42	T2NxMx	Grade 2	clear cell
70	F	55	T1bNxMx	Grade 1	clear cell
72	M	58	T3aN0M0	Grade 2	clear cell
73	F	56	T1bN0M0	Grade 2	papillary
74	M	73	T1bNxMx	Grade 2	clear cell
75	F	65	T1bNoMx	Grade 2	clear cell
76	M	67	T1bNxMx	Grade 3	clear cell
77	F	61	T1bNxMx	Grade 3	clear cell
78	F	49	T2NxMx	Grade 3	papillary
83	M	52	T3aNxMx	Grade 3	clear cell
84	M	67	-	Grade 3	papillary

Table A.2. Expression values of TG2, Syndecan-4 and Integrin β1 in RCC patients:

Patient Code	TG2/18SrRNA tumor/healthy tissue	Syndecan-4/18SrRNA tumor/healthy tissue	Integrin β1/18SrRNA tumor/healthy tissue
1	0,198462	0,314495	0,362395
3	0,167707	0,78229	0,717527
5	2,820988	1,956402	5,668512
6	0,755108	1,053879	0,529735
7	1,977346	0,893728	1,349228
10	0,799338	1,342917	0,641539
11	0,050135	2,655408	0,126472
12	1,889884	1,52338	2,805483
13	0,93039	2,648442	1,640589

Table A.2. Expression values of TG2, Syndecan-4 and Integrin β1 in RCC patients: (continue)

14	2,457869	1,063362	1,296114
15	1,641612	1,083951	2,69186
16	1,584482	4,169436	5,083999
19	0,466779	1,284137	0,787879
21	1,81177	0,791247	0,943673
25	2,928506	1,075353	4,023406
27	0,075885	0,68501	0,784261
30	0,140747	0,342524	0,086271
34	0,456951	2,428468	4,564027
35	0,332852	1,001267	0,417436
36	0,845713	1,269848	0,981878
37	0,185885	0,194815	0,231269
39	0,131901	0,274472	0,114729
40	3,11236	1,74685	1,434715
41	5,336264	1,119871	1,266613
42	0,083716	0,194696	0,01726
43	1,404215	1,922801	0,039367
44	1,454396	0,717985	1,568683
45	0,391774	1,090453	1,094539
46	1,374137	0,652533	0,745231
47	0,246379	0,393539	0,463593
48	0,719973	1,472629	2,327578
49	0,168998	1,124711	1,693141
50	0,002566	0,010795	0,452084
51	0,188825	0,35622	0,824179
52	4,280704	1,082707	1,312976
53	1,334007	1,047178	1,538692
54	0,035066	0,6323	0,774202
55	2,180308	2,898981	1,057118
56	2,933376	2,128231	5,038058
57	0,144859	0,761929	0,519745
58	1,736363	2,639432	1,42948
60	0,292509	0,067888	0,32947
61	0,017743	1,424257	2,363528
62	0,032226	0,060025	0,955455
63	0,074727	0,129926	0,409102
64	0,066198	0,48174	0,893939
65	1,106716	1,03374	0,975651
66	0,063185	1,727459	0,877016
67	0,783767	1,315135	0,7543

Table A.2. Expression values of TG2, Syndecan-4 and Integrin β1 in RCC patients: (continue)

68	0,040395	0,339316	0,38533
69	0,770328	0,171975	0,382381
70	2,102715	1,365829	1,340371
72	0,101131	0,240973	0,490003
73	0,247365	1,034653	0,551504
74	0,364554	0,764967	0,569359
75	0,331018	0,298655	0,468733
76	0,163093	0,433674	1,935225
77	1,032629	5,683629	1,586652
78	0,244991	0,388094	2,812917
83	0,26052	0,995489	4,121492
84	0,095975	0,803718	1,565114

Figure A.1. Statistical Analysis of Figure 4.1. The screen view of MedCalc Statistical Software (CTR = control (healthy) tissues, TM = tumor tissues)

Wilcoxon test (paired samples)

Sample 1	
Variable	Group 1 average TG2 exp in CTR
Sample 2	
Variable	Group 1 average TG2 exp in TM

	Sample 1	Sample 2
Sample size	40	40
Lowest value	0,0000003129	0,00000004127
Highest value	0,07146	0,04091
Median	0,01789	0,002892
95% CI for the median	0,01039 to 0,03560	0,001126 to 0,008128
Interquartile range	0,006846 to 0,03964	0,0005571 to 0,01366

Wilcoxon test (paired samples)

Number of positive differences	2
Number of negative differences	38
Large sample test statistic Z	5,053928
Two-tailed probability	P < 0,0001

Figure A.1. Statistical Analysis of Figure 4.1. The screen view of MedCalc Statistical Software (CTR = control (healthy) tissues, TM = tumor tissues) (continue)

Wilcoxon test (paired samples)

Sample 1	
Variable	Group 2 average TG2 exp in CTR
Sample 2	
Variable	Group 2 average TG2 exp in TM

	Sample 1	Sample 2
Sample size	21	21
Lowest value	0,0009965	0,001601
Highest value	0,07367	0,1457
Median	0,01542	0,01838
95% CI for the median	0,004070 to 0,02010	0,01115 to 0,04227
Interquartile range	0,003817 to 0,02387	0,009719 to 0,04724

Wilcoxon test (paired samples)

Number of positive differences	20
Number of negative differences	1
Large sample test statistic Z	-3,910236
Two-tailed probability	P = 0,0001

Mann-Whitney test (independent samples)

Sample 1	
Variable	Group 1 average TG2 exp in TM
Sample 2	
Variable	Group 2 average TG2 exp in TM

	Sample 1	Sample 2
Sample size	40	21
Lowest value	0,00000004127	0,001601
Highest value	0,04091	0,1457
Median	0,002892	0,01838
95% CI for the median	0,001126 to 0,008128	0,01115 to 0,04227
Interquartile range	0,0005571 to 0,01366	0,009719 to 0,04724

Mann-Whitney test (independent samples)

Average rank of first group	24,6750
Average rank of second group	43,0476
Mann-Whitney U	167,00
Large sample test statistic Z	3,840
Two-tailed probability	P = 0,0001

Figure A.2. Statistical Analysis of Figure 4.2. The screen view of MedCalc Statistical Software (CTR = control (healthy) tissues, TM = tumor tissues)

Wilcoxon test (paired samples)

Sample 1	
Variable	Group 1 average SDC4 exp in CTR
Sample 2	
Variable	Group 1 average SDC4 exp in TM

	Sample 1	Sample 2
Sample size	29	29
Lowest value	0,0000001196	0,00000002328
Highest value	0,1147	0,03641
Median	0,005796	0,002457
95% CI for the median	0,002932 to 0,009963	0,001141 to 0,003674
Interquartile range	0,002322 to 0,01492	0,0008440 to 0,005866

Wilcoxon test (paired samples)

Number of positive differences	0
Number of negative differences	29
Large sample test statistic Z	4,703046
Two-tailed probability	P < 0,0001

Wilcoxon test (paired samples)

Sample 1	
Variable	Group 2 average SDC4 exp in CTR
Sample 2	
Variable	Group 2 average SDC4 exp in TM

	Sample 1	Sample 2
Sample size	32	32
Lowest value	0,0002922	0,0003813
Highest value	0,1211	0,1469
Median	0,01616	0,02745
95% CI for the median	0,006671 to 0,02555	0,009397 to 0,03539
Interquartile range	0,003465 to 0,02901	0,007126 to 0,03864

Wilcoxon test (paired samples)

Number of positive differences	29
Number of negative differences	3
Large sample test statistic Z	-4,188563
Two-tailed probability	P < 0,0001

Figure A.2. Statistical Analysis of Figure 4.2. The screen view of MedCalc Statistical Software (CTR = control (healthy) tissues, TM = tumor tissues) (continue)

Mann-Whitney test (independent samples)

Sample 1	
Variable	Group 1 average SDC4 exp in TM
Sample 2	
Variable	Group 2 average SDC4 exp in TM

	Sample 1	Sample 2
Sample size	29	32
Lowest value	0,00000002328	0,0003813
Highest value	0,03641	0,1469
Median	0,002457	0,02745
95% CI for the median	0,001141 to 0,003674	0,009397 to 0,03539
Interquartile range	0,0008440 to 0,005866	0,007126 to 0,03864

Mann-Whitney test (independent samples)

Average rank of first group	20,1034
Average rank of second group	40,8750
Mann-Whitney U	148,00
Large sample test statistic Z	4,564
Two-tailed probability	P < 0,0001

Figure A.3. Statistical Analysis of Figure 4.3. The screen view of MedCalc Statistical Software (CTR = control (healthy) tissues, TM = tumor tissues)

Wilcoxon test (paired samples)

Sample 1	
Variable	Group 1 average ITGB1 exp in CTR
Sample 2	
Variable	Group 1 average ITGB1 exp in TM

	Sample 1	Sample 2
Sample size	34	34
Lowest value	0,00005671	0,00001114
Highest value	0,2215	0,2024
Median	0,01217	0,005490
95% CI for the median	0,003804 to 0,03182	0,001580 to 0,009882
Interquartile range	0,001556 to 0,04350	0,0002944 to 0,01756

Wilcoxon test (paired samples)

Number of positive differences	1
Number of negative differences	33
Large sample test statistic Z	4,915248
Two-tailed probability	P < 0,0001

Figure A.3. Statistical Analysis of Figure 4.3. The screen view of MedCalc Statistical Software (CTR = control (healthy) tissues, TM = tumor tissues) (continue)

Wilcoxon test (paired samples)

Sample 1	
Variable	Group 2 average ITGB1 exp in CTR
Sample 2	
Variable	Group 2 average ITGB1 exp in TM

	Sample 1	Sample 2
Sample size	27	27
Lowest value	0,0001188	0,0004778
Highest value	0,3790	0,5951
Median	0,009733	0,01554
95% CI for the median	0,002897 to 0,02227	0,005169 to 0,03180
Interquartile range	0,001809 to 0,03175	0,004639 to 0,04932

Wilcoxon test (paired samples)

Number of positive differences	24
Number of negative differences	3
Large sample test statistic Z	-4,156325
Two-tailed probability	P < 0,0001

Mann-Whitney test (independent samples)

Sample 1	
Variable	Group 1 average ITGB1 exp in TM
Sample 2	
Variable	Group 2 average ITGB1 exp in TM

	Sample 1	Sample 2
Sample size	34	27
Lowest value	0,00001114	0,0004778
Highest value	0,2024	0,5951
Median	0,005490	0,01554
95% CI for the median	0,001580 to 0,009882	0,005169 to 0,03180
Interquartile range	0,0002944 to 0,01756	0,004639 to 0,04932

Mann-Whitney test (independent samples)

Average rank of first group	25,0588
Average rank of second group	38,4815
Mann-Whitney U	257,00
Large sample test statistic Z	2,933
Two-tailed probability	P = 0,0034

Figure A.4. Statistical Analysis of Figure 4.4. The screen view of MedCalc Statistical Software (CTR = control (healthy) tissues, TM = tumor tissues)

Mann-Whitney test (independent samples)

Sample 1	
Variable	Group 1 average TG2 TM/CTR
Sample 2	
Variable	Group 2 average TG2 TM/CTR

	Sample 1	Sample 2
Sample size	44	17
Lowest value	0,002566	1,0326
Highest value	1,9773	5,3363
Median	0,2217	2,1027
95% CI for the median	0,1455 to 0,3328	1,5854 to 2,9268
Interquartile range	0,08985 to 0,5934	1,5394 to 2,9297

Mann-Whitney test (independent samples)

Average rank of first group	23,0000
Average rank of second group	51,7059
Mann-Whitney U	22,00
Large sample test statistic Z	5,662
Two-tailed probability	P < 0,0001

Mann-Whitney test (independent samples)

Sample 1	
Variable	Group 1 average SDC4 TM/CTR
Sample 2	
Variable	Group 2 average SDC4 TM/CTR

	Sample 1	Sample 2
Sample size	44	17
Lowest value	0,01079	1,0337
Highest value	2,6554	5,6836
Median	0,7400	1,5234
95% CI for the median	0,3949 to 0,9920	1,0827 to 2,1255
Interquartile range	0,3269 to 1,1076	1,0809 to 2,2560

Mann-Whitney test (independent samples)

Average rank of first group	24,9773
Average rank of second group	46,5882
Mann-Whitney U	109,00
Large sample test statistic Z	4,263
Two-tailed probability	P < 0,0001

Figure A.5. Statistical Analysis of Figure 4.5. The screen view of MedCalc Statistical Software (CTR = control (healthy) tissues, TM = tumor tissues)

Mann-Whitney test (independent samples)

Sample 1	
Variable	Group 1 average TG2 TM/CTR
Sample 2	
Variable	Group 2 average TG2 TM/CTR

	Sample 1	Sample 2
Sample size	43	18
Lowest value	0,002566	1,0326
Highest value	1,4042	5,3363
Median	0,1985	2,0400
95% CI for the median	0,1433 to 0,3317	1,6793 to 2,8858
Interquartile range	0,08678 to 0,4643	1,6416 to 2,9285

Mann-Whitney test (independent samples)

Average rank of first group	22,1163
Average rank of second group	52,2222
Mann-Whitney U	5,00
Large sample test statistic Z	6,041
Two-tailed probability	P < 0,0001

Mann-Whitney test (independent samples)

Sample 1	
Variable	Group 1 average ITGB1 TM/CTR
Sample 2	
Variable	Group 2 average ITGB1 TM/CTR

	Sample 1	Sample 2
Sample size	43	18
Lowest value	0,01726	0,9437
Highest value	4,5640	5,6685
Median	0,7175	1,4867
95% CI for the median	0,4817 to 0,8448	1,3239 to 2,7603
Interquartile range	0,4112 to 0,9803	1,3130 to 2,8055

Mann-Whitney test (independent samples)

Average rank of first group	24,7674
Average rank of second group	45,8889
Mann-Whitney U	119,00
Large sample test statistic Z	4,238
Two-tailed probability	P < 0,0001

Figure A.6. Statistical Analysis of Figure 4.7. The screen view of GraphPad Prism (CTR = control (healthy) tissues, TM = tumor tissues)

Table Analyzed	Data 1
Column C	50 CTR
vs	vs
Column D	50 TM
Paired t test	
P value	0,0099
P value summary	**
Are means signif. different? (P < 0.05)	Yes
One- or two-tailed P value?	Two-tailed
t, df	t=9,955 df=2
Number of pairs	3

Table Analyzed	Data 1
Column O	68 CTR
vs	vs
Column P	68 TM
Paired t test	
P value	0,0241
P value summary	*
Are means signif. different? (P < 0.05)	Yes
One- or two-tailed P value?	Two-tailed
t, df	t=4,237 df=3
Number of pairs	4

Table Analyzed	Data 1
Column G	60 CTR
vs	vs
Column H	60 TM
Paired t test	
P value	0,0037
P value summary	**
Are means signif. different? (P < 0.05)	Yes
One- or two-tailed P value?	Two-tailed
t, df	t=8,307 df=3
Number of pairs	4

Table Analyzed	Data 1
Column Q	73 CTR
vs	vs
Column R	73 TM
Paired t test	
P value	0,001
P value summary	***
Are means signif. different? (P < 0.05)	Yes
One- or two-tailed P value?	Two-tailed
t, df	t=13,15 df=3
Number of pairs	4

Table Analyzed	Data 1
Column I	63 CTR
vs	vs
Column J	63 TM
Paired t test	
P value	0,0051
P value summary	**
Are means signif. different? (P < 0.05)	Yes
One- or two-tailed P value?	Two-tailed
t, df	t=13,91 df=2
Number of pairs	3

Table Analyzed	Data 1
Column S	74 CTR
vs	vs
Column T	74 TM
Paired t test	
P value	< 0,0001
P value summary	***
Are means signif. different? (P < 0.05)	Yes
One- or two-tailed P value?	Two-tailed
t, df	t=29,21 df=3
Number of pairs	4

Table Analyzed	Data 1
Column K	64 CTR
vs	vs
Column L	64 TM
Paired t test	
P value	0,01
P value summary	**
Are means signif. different? (P < 0.05)	Yes
One- or two-tailed P value?	Two-tailed
t, df	t=9,942 df=2
Number of pairs	3

Table Analyzed	Data 1
Column U	75 CTR
vs	vs
Column V	75 TM
Paired t test	
P value	0,0218
P value summary	*
Are means signif. different? (P < 0.05)	Yes
One- or two-tailed P value?	Two-tailed
t, df	t=4,399 df=3
Number of pairs	4

Figure A.6. Statistical Analysis of Figure 4.7. The screen view of GraphPad Prism (CTR = control (healthy) tissues, TM = tumor tissues) (continue)

Table Analyzed	Data 1
Column M	66 CTR
vs	vs
Column N	66 TM
Paired t test	
P value	0,0341
P value summary	*
Are means signif. different? (P < 0.05)	Yes
One- or two-tailed P value?	Two-tailed
t, df	t=5,280 df=2
Number of pairs	3

Table Analyzed	Data 1
Column S	78 CTR
vs	vs
Column T	78 TM
Paired t test	
P value	0,0158
P value summary	*
Are means signif. different? (P < 0.05)	Yes
One- or two-tailed P value?	Two-tailed
t, df	t=4,954 df=3
Number of pairs	4

Figure A.7. Statistical Analysis of Figure 4.8. The screen view of GraphPad Prism (CTR = control (healthy) tissues, TM = tumor tissues)

Table Analyzed	Data 1
Column A	5 CTR
vs	vs
Column B	5 TM
Paired t test	
P value	0,0043
P value summary	**
Are means signif. different? (P < 0.05)	Yes
One- or two-tailed P value?	Two-tailed
t, df	t=15,23 df=2
Number of pairs	3

Table Analyzed	Data 1
Column C	12 CTR
vs	vs
Column D	12 TM
Paired t test	
P value	0,0192
P value summary	*
Are means signif. different? (P < 0.05)	Yes
One- or two-tailed P value?	Two-tailed
t, df	t=7,118 df=2
Number of pairs	3

Table Analyzed	Data 1
Column E	13 CTR
vs	vs
Column F	13 TM
Paired t test	
P value	0,0312
P value summary	*
Are means signif. different? (P < 0.05)	Yes
One- or two-tailed P value?	Two-tailed
t, df	t=5,531 df=2
Number of pairs	3

Table Analyzed	Data 1
Column G	14 CTR
vs	vs
Column H	14 TM
Paired t test	
P value	0,0005
P value summary	***
Are means signif. different? (P < 0.05)	Yes
One- or two-tailed P value?	Two-tailed
t, df	t=46,60 df=2
Number of pairs	3

Figure A.7. Statistical Analysis of Figure 4.8. The screen view of GraphPad Prism (CTR = control (healthy) tissues, TM = tumor tissues) (continue)

Table Analyzed	Data 1
Column I	15 CTR
vs	vs
Column J	15 TM
Paired t test	
P value	0,0003
P value summary	***
Are means signif. different? (P < 0.05)	Yes
One- or two-tailed P value?	Two-tailed
t, df	t=55,01 df=2
Number of pairs	3

Table Analyzed	Data 1
Column K	16 CTR
vs	vs
Column L	16 TM
Paired t test	
P value	0,001
P value summary	***
Are means signif. different? (P < 0.05)	Yes
One- or two-tailed P value?	Two-tailed
t, df	t=31,62 df=2
Number of pairs	3

Table Analyzed	Data 1
Column M	21 CTR
vs	vs
Column N	21 TM
Paired t test	
P value	0,0015
P value summary	**
Are means signif. different? (P < 0.05)	Yes
One- or two-tailed P value?	Two-tailed
t, df	t=25,53 df=2
Number of pairs	3

Table Analyzed	Data 1
Column O	25 CTR
vs	vs
Column P	25 TM
Paired t test	
P value	0,0033
P value summary	**
Are means signif. different? (P < 0.05)	Yes
One- or two-tailed P value?	Two-tailed
t, df	t=17,24 df=2
Number of pairs	3

Table Analyzed	Data 1
Column Q	40 CTR
vs	vs
Column R	40 TM
Paired t test	
P value	0,0005
P value summary	***
Are means signif. different? (P < 0.05)	Yes
One- or two-tailed P value?	Two-tailed
t, df	t=44,27 df=2
Number of pairs	3

Table Analyzed	Data 1
Column S	41 CTR
vs	vs
Column T	41 TM
Paired t test	
P value	0,0007
P value summary	***
Are means signif. different? (P < 0.05)	Yes
One- or two-tailed P value?	Two-tailed
t, df	t=36,70 df=2
Number of pairs	3

Figure A.8. Statistical Analysis of Figure 4.9. The screen view of GraphPad Prism (CTR = control (healthy) tissues, TM = tumor tissues)

Table Analyzed	Data 1		Table Analyzed	Data 1
Column A	RPTEC		Column B	Caki-2
vs	vs		vs	vs
Column C	A-498		Column C	A-498
Unpaired t test			Unpaired t test	
P value	0,0118		P value	0,0219
P value summary	*		P value summary	*
Are means signif. different? (P < 0.05)	Yes		Are means signif. different? (P < 0.05)	Yes
One- or two-tailed P value?	Two-tailed		One- or two-tailed P value?	Two-tailed
t, df	t=9,118 df=2		t, df	t=6,639 df=2

Figure A.9. Statistical Analysis of Figure 4.10. The screen view of GraphPad Prism (CTR = control (healthy) tissues, TM = tumor tissues)

Table Analyzed	Data 1		Table Analyzed	Data 1
Column A	RPTEC		Column B	Caki-2
vs	vs		vs	vs
Column B	Caki-2		Column C	A-498
Unpaired t test			Unpaired t test	
P value	0,0341		P value	0,0132
P value summary	*		P value summary	*
Are means signif. different? (P < 0.05)	Yes		Are means signif. different? (P < 0.05)	Yes
One- or two-tailed P value?	Two-tailed		One- or two-tailed P value?	Two-tailed
t, df	t=5,278 df=2		t, df	t=8,606 df=2

Figure A.10. Statistical Analysis of Figure 4.11. The screen view of GraphPad Prism (CTR = control (healthy) tissues, TM = tumor tissues)

Table Analyzed	Data 1
Column A	RPTEC
vs	vs
Column B	Caki-2
Unpaired t test	
P value	0,0097
P value summary	**
Are means signif. different? (P < 0.05)	Yes
One- or two-tailed P value?	Two-tailed
t, df	t=10,10 df=2

Table Analyzed	Data 1
Column B	Caki-2
vs	vs
Column C	A-498
Unpaired t test	
P value	0,0012
P value summary	**
Are means signif. different? (P < 0.05)	Yes
One- or two-tailed P value?	Two-tailed
t, df	t=28,62 df=2

Table Analyzed	Data 1
Column A	RPTEC
vs	vs
Column C	A-498
Unpaired t test	
P value	0,0031
P value summary	**
Are means signif. different? (P < 0.05)	Yes
One- or two-tailed P value?	Two-tailed
t, df	t=17,84 df=2

Figure A.11. Statistical Analysis of Figure 4.12. The screen view of GraphPad Prism (CTR = control (healthy) tissues, TM = tumor tissues)

Table Analyzed	Data 1
Column A	RPTEC
vs	vs
Column B	Caki-2
Unpaired t test	
P value	< 0,0001
P value summary	***
Are means signif. different? (P < 0.05)	Yes
One- or two-tailed P value?	Two-tailed
t, df	t=15,94 df=6

Table Analyzed	Data 1
Column A	RPTEC
vs	vs
Column C	A-498
Unpaired t test	
P value	< 0,0001
P value summary	***
Are means signif. different? (P < 0.05)	Yes
One- or two-tailed P value?	Two-tailed
t, df	t=11,14 df=6

REFERENCES

1. Reddi, A. S. and K. Kuppasani, "Foundations for Clinical Practice and Overview: Kidney function in health and disease", in L. Byham-Gray, J. D. Burrowes and G. M. Chertow, *Nutrition in Kidney Diseases*, pp. 3-15, Humana Press, Totowa, 2008.

2. P. Patel, and reviewed by D. Zieve and VeriMed Healthcare Network, A.D.A.M., Inc. http://www.adamimages.com/Kidney-anatomy-Illustration/PI294/F3.

3. Briggs, J. P., W. Kriz and J. B. Schnermann, "Overview of Kidney Function and Structure", in A. Greenberg and A. K. Cheung, *Primer on Kidney Diseases*, pp. 2-19, Elsevier Health Sciences, Philadelphia, 2005.

4. O'Callaghan C. and B. M. Brenner, The Kidney at a Glance, Wiley-Blackwell, Oxford, 2000.

5. Muller, M., BIOS 100 Lecture Notes Fall 2004, Lecture Materials Online, http://www.uic.edu/classes/bios/bios100/lecturesf04am/lect21.htm, 2004.

6. Chow W. H., L. M. Dong and S. S. Devesa, "Epidemiology and Risk Factors for Kidney Cancer", *Nature Reviews Urology*, Vol. 7, pp. 245–257, 2010.

7. Homer, M. J., et al. (eds), SEER Cancer Statistics Review, 1975–2006, National Cancer Institute, http://seer.cancer.gov/csr/1975_2006/, 2009.

8. Parkin D. M., F. Bray, J. Ferlay and P. Pisani, "Global cancer statistics, 2002", *CA Cancer Journal for Clinicians*, Vol. 55, No. 2, pp. 74-108, 2005.

9. THE GLOBOCAN PROJECT, GLOBOCAN 2008, World Health Organization, http://globocan.iarc.fr/factsheets/populations/factsheet.asp?uno=792.

10. Ferlay, J., P. Bray, P. Pisani and D. M. Parkin, *GLOBOCAN 2000: Cancer Incidence, Mortality and Prevalence Worldwide*, IARC Press, Lyon, 2001.

11. Rini, B. I., S. C. Campbell and B. Escudier, "Renal Cell Carcinoma", *Lancet*, Vol. 373, No. 9669, pp. 1119-1132, 2009.

12. Kovacs, G., M. Akhtar, B. J. Beckwith, P. Bugert, C. S. Cooper, B. Delahunt, J. N. Eble, S. Fleming, B. Ljungberg, L. J. Medeiros, H. Moch, V. E. Reuter, E. Ritz, G. Roos, D. Schmidt, J. R. Srigley, S. Störkel, E. van den Berg and B, Zbar, "The Heidelberg Classification of Renal Cell Tumours", *The Journal of Pathology*, Vol. 183, No. 2, pp. 131-133, 1997.

13. Cheville, J. C., C. M. Lohse, H. Zincke, A. L. Weaver and M. L. Blute, "Comparisons of Outcome and Prognostic Features Among Histologic Subtypes of Renal Cell Carcinoma", *American Journal Surgical Pathology*, Vol. 27, No. 5, pp. 612-624, 2003.

14. Ljungberg, B., N. C. Cowan, D. C. Hanbury, M. Hora, M. A. Kuczyk, A. S. Merseburger, J. J. Patard, P. F. Mulders and I. C. Sinescu, European Association of Urology Guideline Group, "EAU Guidelines on Renal Cell Carcinoma: The 2010 Update", *European Urology*, Vol. 58, No. 3, pp. 398-406, 2010.

15. Delahunt, B., "Advances and Controversies In Grading and Staging of Renal Cell Carcinoma", *Modern Pathology*, Vol. 22, pp. 24-36, 2009.

16. Suárez, C., R. Morales, E. Muñoz, J. Rodón, C. M. Valverde and J. Carles, "Molecular Basis for the Treatment of Renal Cell Carcinoma", *Clinical & Translational Oncology*, Vol. 12, No. 1, pp. 15-21, 2010.

17. Lorand, L. and S. M. Conrad, "Transglutaminases", *Molecular and Cellular Biochemistry*, Vol. 58 No. 1, pp. 9-35, 1984.

18. Pisano J. J., J. S. Finlayson, M. P. Peyton, "Cross-link in fibrin polymerized by factor 13: epsilon-(gamma-glutamyl)lysine", *Science*, Vol. 160, No. 830, pp. 892-893, 1968.

19. Lorand, L. and R. M. Graham, "Transglutaminases: Crosslinking Enzymes with Pleiotropic Functions", *Molecular and Cellular Biochemistry*, Vol. 4, No. 2, pp. 140-156, 2003.

20. Folk, J. E., J. P. Mullooly, P. W. Cole, "Mechanism of Action of Guinea Pig Liver Transglutaminase. II. The Role of Metal in Enzyme Activation", *The Journal of Biological Chemistry*, Vol. 242, No. 8, pp. 1838-1844, 1967.

21. Griffin, M. and J. Wilson, "Detection of Epsilon(gamma-glutamyl) Lysine", *Molecular and Cellular Biochemistry*, Vol. 58, No. 1-2, pp. 37-49, 1984.

22. Birckbichler, P. J., G. R. Orr, H. A. Carter, M. K. Jr Patterson, "Catalytic formation of Epsilon-(Gamma-Glutamyl)lysine in Guinea Pig Liver Transglutaminase", *Biochemical and Biophysical Research Communications*, Vol. 78, No. 1, pp. 1-7, 1977.

23. Folk, J. E. and J. S. Finlaysaon, "The Epsilon-(gamma-glutamyl)lysine Crosslink and the Catalytic Role of Transglutaminases", *Advances in Protein Chemistry*, Vol. 31, pp. 1-133, 1977.

24. Mycek, M. J. and H. Waelsch, "The Enzymatic Deamidation of Proteins", *The Journal of Biological Chemistry*, Vol. 235, pp. 3513-3517, 1960.

25. Parameswaran, K. N., X. F. Cheng, E. C. Chen, P. T. Velasco, J. H. Wilson and L. Lorand, "Hydrolysis of Gamma:epsilon Isopeptides by Cytosolic Transglutaminases and by Coagulation Factor XIIIa", *The Journal of Biological Chemistry*, Vol. 272, No. 25, pp. 10311-10317, 1997.

26. Thomázy, V. and L. Fésüs, "Differential Expression of Tissue Transglutaminase in Human Cells. An Immunohistochemical Study", *Cell and Tissue Research*, Vol. 255, No. 1, pp. 215-224, 1989.

27. Lee, K. N., P. J. Birckbichler and M. K. Jr Patterson, "GTP Hydrolysis by Guinea Pig Liver Transglutaminase", *Biochemical and Biophysical Research Communications*, Vol. 162, No. 3, pp. 1370-1375, 1989.

28. Lai, T. S., A. Bielawska, K. A. Peoples, Y. A. Hannun and C. S. Greenberg, "Sphingosylphosphocholine Reduces the Calcium Ion Requirement for Activating Tissue Transglutaminase", *The Journal of Biological Chemistry*, Vol. 272, No. 26, pp. 16295-16300, 1997.

29. Achyuthan, K. E. and C. S. Greenberg, "Identification of a Guanosine Triphosphate-Binding Site on Guinea Pig Liver Transglutaminase. Role of GTP and Calcium Ions in Modulating Activity", *The Journal of Biological Chemistry*, Vol. 262, No. 4, pp. 1901-1906, 1987.

30. Hasegawa, G., M. Suwa, Y. Ichikawa, T. Ohtsuka, S. Kumagai, M. Kikuchi, Y. Sato and Y. Saito, "A Novel Function of Tissue-Type Transglutaminase: Protein Disulphide Isomerase", *Biochemical Journal*, Vol. 373, No. 3, pp. 793-803, 2003.

31. Mishra, S. and L. J. Murphy, "Tissue Transglutaminase Has Intrinsic Kinase Activity: Identification of Transglutaminase 2 as an Insulin-Like Growth Factor-Binding Protein-3 Kinase", *The Journal of Biological Chemistry*, Vol. 279, No. 23, pp. 23863-23868, 2004.

32. Mishra, S. and L. J. Murphy, "The p53 Oncoprotein Is a Substrate for Tissue Transglutaminase Kinase Activity", *Biochemical and Biophysical Research Communications*, Vol. 339, No. 2, pp. 726-730, 2006.

33. Mishra, S., G. Melino, and L. J. Murphy, "Transglutaminase 2 Kinase Activity Facilitates Protein Kinase A-Induced Phosphorylation of Retinoblastoma Protein", *The Journal of Biological Chemistry*, Vol. 282, No. 25, pp. 18108-18115, 2007.

34. Griffin, M., R. Casadio, and C. M. Bergamini, "Transglutaminases: Nature's Biological Glues", *Biochemical Journal*, Vol. 368, No. 2, pp. 377-396, 2002.

35. Smethurst, P. A. and M. Griffin, "Measurement of Tissue Transglutaminase Activity in a Permeabilized Cell System: Its Regulation by Ca^{2+} and nucleotides", *Biochemical Journal*, Vol. 313, No. 3, pp. 803-808, 1996.

36. Nunes, I., P. E. Gleizes, C. N. Metz and D. B. Rifkin, "Latent Transforming Growth Factor-Beta Binding Protein Domains Involved in Activation and Transglutaminase-Dependent Cross-Linking of Latent Transforming Growth Factor-beta", *The Journal of Cell Biology*, Vol. 136, No. 5, pp. 1151-1163, 1997.

37. Casini, A., M. Pinzani, S. Milani, C. Grappone, G. Galli, A. M. Jezequel, D. Schuppan, C. M. Rotella and C. Surrenti, "Regulation of Extracellular Matrix Synthesis by Transforming Growth Factor Beta 1 in Human Fat-Storing Cells", *Gastroenterology*, Vol. 105, No. 1, pp. 245-253, 1993.

38. Li, J. H., X. R. Huang H. J. Zhu, R. Johnson and H. Y. Lan, "Role of TGF-beta Signaling in Extracellular Matrix Production Under High Glucose Conditions", *Kidney International*, Vol. 63, No. 6, pp. 2010-2019, 2003.

39. Verderio, E., C. Gaudry, S. Gross, C. Smith, S. Downes and M. Griffin, "Regulation of Cell Surface Tissue Transglutaminase: Effects on Matrix Storage of Latent Transforming Growth Factor-beta Binding Protein-1", *Journal of Histochemistry and Cytochemistry*, Vol. 47, No. 11, pp. 1417-1432, 1999.

40. Douthwaite, J. A., T. S. Johnson, J. L. Haylor, P. Watson and A. M. El Nahas, "Effects of Transforming Growth Factor-beta1 on Renal Extracellular Matrix

Components and Their Regulating Proteins", *Journal of the American Society of Nephrology*, Vol. 10, No. 10, pp. 2109-19, 1999.

41. Akimov, S. S., D. Krylov, L. F. Fleischman and A. M. Belkin, "Tissue Transglutaminase is an Integrin-Binding Adhesion Coreceptor for Fibronectin", *The Journal of Cell Biology*, Vol. 148, No. 4, pp. 825-838, 2000.

42. Telci, D., Z. Wang, X. Li, E. A. Verderio, M. J. Humphries, M. Baccarini, H. Basaga and M. Griffin, "Fibronectin-Tissue Transglutaminase Matrix Rescues RGD-Impaired Cell Adhesion Through Syndecan-4 and Beta1 Integrin Co-signaling", *The Journal of Biological Chemistry*, Vol. 283, No. 30, pp. 20937-20947, 2008.

43. Telci, D. and M. Griffin, "Tissue transglutaminase (TG2)--A Wound Response Enzyme", *Front Bioscience*, Vol. 11, pp. 867-882, 2006.

44. Mosher, D. F., "Physiology of Fibronectin", *The Annual Review of Medicine*, Vol. 35, pp. 561-575, 1984.

45. Schwarzbauer, J. E. and J. L. Sechler, "Fibronectin fibrillogenesis: A Paradigm for Extracellular Matrix Assembly", *Current Opinion in Cell* Biology, Vol. 11 No. 5, pp. 622-627, 1999.

46. Fogerty, F. J., S. K. Akiyama, K. M. Yamada and D. F. Mosher, "Inhibition of Binding of Fibronectin to Matrix Assembly Sites by Anti-Integrin (alpha 5 beta 1) Antibodies", *The Journal of Cell Biology*, Vol. 111, No. 2, pp. 699-708, 1990.

47. Alberts B., A. Johnson, J. Lewis, M. Rafi, K. Roberts and P. Walter, "Mechanisms of Cell Communication", in *The Molecular Biology of the Cell, Fifth Edition*, Garland Science, New York, 2008.

48. Burridge, K. and M. Chrzanowska-Wodnicka, "Focal Adhesions, Contractility, and Signaling", *Annual Review of Cell and Developmental Biology*, Vol. 12, pp. 463-518, 1996.

49. Giancotti, F. G. and E. Ruoslahti, "Integrin signaling", *Science*, Vol. 285, No. 5430, pp. 1028-1032, 1999.

50. Hynes, R. O., "Integrins: Bidirectional, Allosteric Signaling Machines", *Cell*, Vol. 110, No. 6, pp. 673-687, 2002.

51. Humphries, M. J., "Integrin Structure", *Biochemical Society Transactions*, Vol. 28, No. 4, pp. 311-339, 2000.

52. Gailit, J. and E. Ruoslahti, "Regulation of the Fibronectin Receptor Affinity by Divalent Cations", *The Journal of Biological Chemistry*, Vol. 263, No. 26, pp. 12927-12932, 1988.

53. Gulino, D., C. Boudignon, L. Y. Zhang, E. Concord, M. J. Rabiet and G. Marguerie, "Ca(2+)-binding Properties of the Platelet Glycoprotein IIb Ligand-Interacting Domain", *The Journal of Biological Chemistry*, Vol. 267, No. 2, pp. 1001-1007, 1992.

54. Smith, J. W. and D. A. Cheresh, "Labeling of Integrin Alpha v Beta 3 with 58Co(III). Evidence of Metal Ion Coordination Sphere Involvement in Ligand Binding", *The Journal of Biological Chemistry*, Vol. 266, No. 18, pp. 11429-11432, 1991.

55. O'Toole, T. E., Y. Katagiri, R. J. Faull, K. Peter, R. Tamura, V. Quaranta, J. C. Loftus, S. J. Shattil and M. H. Ginsberg, "Integrin Cytoplasmic Domains Mediate Inside-Out Signal Transduction", *The Journal of Cell Biology*, Vol. 124, No. 6, pp. 1047-1059, 1994.

56. Schwartz, M. A., M. D. Schaller and M. H. Ginsberg, "Integrins: Emerging Paradigms of Signal Transduction", *Annual Review of Cell and Developmental Biology*, Vol. 11, pp. 549-599, 1995.

57. Liu, S., D. A. Calderwood and M. H. Ginsberg, "Integrin Cytoplasmic Domain-Binding Proteins", *Journal of Cell Science*, Vol. 113, No. 20, pp. 3563-3571, 2000.

58. Woods, A. and J. R. Couchman, "Syndecans: Synergistic Activators of Cell Adhesion", *Trends in Cell Biology*, Vol. 8, No. 5, pp. 189-192, 1998.

59. Lambaerts, K., S. A. Wilcox-Adelman and P. Zimmermann, "The Signaling Mechanisms of Syndecan Heparan Sulfate Proteoglycans", *Current Opinion in Cell Biology*, Vol. 21, No. 5, pp. 662-669, 2009.

60. Carey, D. J., "Syndecans: Multifunctional Cell-Surface Co-receptors", *Biochemical Journal*, Vol. 327, pp. 1-16, 1997.

61. Woods, A. and J. R. Couchman, "Syndecan-4 and focal adhesion function", *Current Opinion in Cell Biology*, Vol. 13, No. 5, pp. 578-583, 2001.

62. Piacentini, M., L. Piredda, D. Starace, M. Annicchiarico-Petruzzelli, M. Mattei, S. Oliverio, M. Grazia Farrace, and G. Melino, "Differential Growth of N- And S-Type Human Neuroblastoma Cells Xenografted into Scid Mice. Correlation with Apoptosis", *The Journal of Pathology*, Vol. 180, No. 4, pp. 415-422, 1996.

63. Nicholas, B., P. Smethurst, E. Verderio, R. Jones and M. Griffin, "Cross-linking of Cellular Proteins by Tissue Transglutaminase During Necrotic Cell Death: A Mechanism for Maintaining Tissue Integrity", *Biochemical Journal*, Vol. 371, pp. 413-422, 2003.

64. Mehta, K., "High Levels of Transglutaminase Expression in Doxorubicin-Resistant Human Breast Carcinoma Cells", *International Journal of Cancer*, Vol. 58, No. 3, pp. 400-406, 1994.

65. Birckbichler, P. J. and M. K. Jr. Patterson, "Cellular Transglutaminase, Growth, and Transformation", *Annals of the New York Academy of Sciences*, Vol. 312, pp. 354-365, 1978.

66. Mian, S., "The Importance of the GTP-binding Protein Tissue Transglutaminase in the Regulation of Cell Cycle Progression", *FEBS Letters*, Vol. 370, No. 1-2, pp. 27-31, 1995.

67. Oliverio, S., A. Amendola, F. Di Sano, M. G. Farrace, L. Fesus, Z. Nemes, L. Piredda, A. Spinedi and M. Piacentini, "Tissue Transglutaminase-dependent Posttranslational Modification of the Retinoblastoma Gene Product in Promonocytic Cells Undergoing Apoptosis", *Molecular and Cellular Biology*, Vol. 17, No. 10, pp. 6040-6048, 1997.

68. Mann, A. P., A. Verma, G. Sethi, B. Manavathi, H. Wang, J. Y. Fok, A. B. Kunnumakkara, R. Kumar, B. B. Aggarwal, and K. Mehta, "Overexpression of Tissue Transglutaminase Leads to Constitutive Activation of Nuclear Factor-kappaB in Cancer Cells: Delineation of a Novel Pathway", *Cancer Research*, Vol. 66, No. 17, pp. 8788-8795, 2006.

69. Ruddon, R.W., "The Biochemistry and Cell Biology of Cancer" in *Cancer Biology, Fourth Edition*, pp. 117-257, Oxford University Press, New York, 2007.

70. Kotsakis, P., and M. Griffin, "Tissue Transglutaminase in Tumour Progression: Friend or Foe?", *Amino Acids*, Vol. 33, No. 2, pp. 373-384, 2007.

71. Mehta, K., A. Kumar, and H. I. Kim, "Transglutaminase 2: a Multi-tasking Protein in the Complex Circuitry of Inflammation and Cancer", *Biochemical Pharmacology*, Vol. 80, No. 12, pp. 1921-1929, 2010.

72. Mehta, K., J. Fok, F. R. Miller, D. Koul and A. A. Sahin, "Prognostic Significance of Tissue Transglutaminase in Drug Resistant and Metastatic Breast Cancer", *Clinical Cancer Research*, Vol. 10, No. 23, pp. 8068-8076, 2004.

73. Herman, J. F., L. S. Mangala and K. Mehta, "Implications of Increased Tissue Transglutaminase (TG2) Expression in Drug-resistant Breast Cancer (MCF-7) Cells", *Oncogene*, Vol. 25, No. 21, pp. 3049-3058, 2006.

74. Mangala, L. S., J. Y. Fok, I. R. Zorrilla-Calancha, A. Verma and K. Mehta, "Tissue Transglutaminase Expression Promotes Cell Attachment, Invasion and Survival in Breast Cancer Cells", *Oncogene*, Vol. 26, No. 17, pp. 2459-2470, 2006.

75. Fok, J. Y., S. Ekmekcioglu and K. Mehta, "Implications of Tissue Transglutaminase Expression in Malignant Melanoma", *Molecular Cancer Therapeutics*, Vol. 5, No. 6, pp. 1493-1503, 2006.

76. Verma, A., H. Wang, B. Manavathi, J. Y. Fok, A. P. Mann, R. Kumar and K. Mehta, "Increased Expression of Tissue Transglutaminase in Pancreatic Ductal Adenocarcinoma and Its Implications in Drug Resistance and Metastasis", *Cancer Research*, Vol. 66, No. 21, pp. 10525-10533, 2006.

77. Belkin, A. M., S. S. Akimov, L. S. Zaritskaya, B. I. Ratnikov, E. I. Deryugina and A. Y. Strongin, "Matrix-dependent Proteolysis of Surface Transglutaminase by Membrane-type Metalloproteinase Regulates Cancer Cell Adhesion and Locomotion", *The Journal of Biological Chemistry*, Vol. 276, No. 21, pp. 18415-18422, 2001.

78. Bell, S. E., A. Mavila, R. Salazar, K. J. Bayless, S. Kanagala, S. A. Maxwell, and G. E. Davis, "Differential Gene Expression during Capillary Morphogenesis in 3D Collagen Matrices: Regulated Expression of Genes Involved in Basement Membrane Matrix Assembly, Cell Cycle Progression, Cellular Differentiation and G-protein Signaling", *Journal of Cell Science*, Vol. 114, pp. 2755-2773, 2001.

79. Jones, R. A., P. Kotsakis, T. S. Johnson, D. Y. Chau, S. Ali, G. Melino and M. Griffin, "Matrix Changes Induced by Transglutaminase 2 Lead to Inhibition of Angiogenesis And Tumor Growth", *Cell Death and Differentiation*, Vol. 13, No. 9, pp. 1442-1453, 2006.

80. Schaeffer, W. I., Mammalian Cell Culture in Molecular Biology, University of Vermont, http://www.uvm.edu/~wschaeff/BasicCulture1.html.

81. Matrisian, L. M., "Metalloproteinases and Their Inhibitors in Matrix Remodeling", *Trends in Genetics*, Vol. 6, No. 4, pp. 121-125, 1990.

82. Ritter, S. J. and P. J. Davies, "Identification of a Transforming Growth Factor-Beta1/bone Morphogenetic Protein 4 (TGF-beta1/BMP4) Response Element within the Mouse Tissue Transglutaminase Gene Promoter", *The Journal of Biological Chemistry*, Vol. 273, No. 21, pp. 12798-12806, 1998.

83. Mangala, L. S., B. Arun, A. A. Sahin and K. Mehta, "Tissue Transglutaminase-induced Alterations in Extracellular Matrix Inhibit Tumor Invasion", *Molecular Cancer*, Vol. 4, No. 33, 2005.

84. Birckbichler, P. J., R. B. Bonner, R. E. Hurst, B. L. Bane, J. V. Pitha and G. P. Hemstreet 3rd, "Loss of Tissue Transglutaminase as a Biomarker for Prostate Adenocarcinoma", *Cancer*, Vol. 89, No. 2, pp. 412-423, 2000.

85. Akimov, S. S. and A. M. Belkin, "Cell-surface Transglutaminase Promotes Fibronectin Assembly via Interaction with the Gelatin-binding Domain of Fibronectin: a Role in TGFbeta-dependent Matrix Deposition", *Journal of Cell Science*, Vol. 114, pp. 2989-3000, 2001.

86. Verderio, E. A., D. Telci, A. Okoye, G. Melino and M. Griffin, "A Novel RGD-independent Cell Adhesion Pathway Mediated by Fibronectin-bound Tissue Transglutaminase Rescues Cells from Anoikis", *The Journal of Biological Chemistry.*, Vol. 278, No. 43, pp. 42604-42614, 2003.

87. Strefford, J. C., I. Stasevich, T. M. Lane, Y. J. Lu, T. Oliver and B. D. Young, "A Combination of Molecular Cytogenetic Analyses Reveals Complex Genetic Alterations in Conventional Renal Cell Carcinoma", *Cancer Genetics and Cytogenetics*, Vol. 159, No. 1, pp. 1-9, 2005.